

1 **BORIS-2 – a benthic ecosystem model based on allometry**

2 Adrian P. Martin¹, [Anieke Brombacher¹](#), Noëlie Benoist¹, Brian J. Bett¹, ~~Anieke Brombacher¹~~, Jennifer
3 M. Durden¹, Sophy Oliver¹, Andrew Yool¹

4 ¹National Oceanography Centre, Southampton, SO14 3ZH, UK

5 *Correspondence to:* Adrian P. Martin (adrian.martin@noc.ac.uk)

6 **Abstract.** We present a model describing the population dynamics of benthic biota, feeding from a common resource that is
7 supplied by a flux of sinking organic carbon arriving on the seafloor. By using allometric relationships for the physiological
8 processes of growth, mortality and respiration, and for food limitation, the model represents the population dynamics of
9 organisms ranging in size from bacteria (10^{-14} g wet weight C) to large metazoans (10^3 gwwt C). The effect of temperature on
10 physiological rates is also included. The only forcing information required is the ambient temperature and the rate of supply
11 of sinking organic carbon. The model can be used for, and tuned to, specific locations. However, a parameter set is provided
12 that is generally applicable. The ability of the model to simultaneously reproduce biomass size distributions at five contrasting
13 sites is demonstrated for this parameter set. Other examples of use are also shown, using the model to explore global patterns
14 of benthic biomass, and responding to a change in food supply.

15 **1 Introduction**

16 The surface ocean, or epipelagic, ecosystem has received considerable attention from modellers for a variety of reasons,
17 spanning from the magnitude of biogeochemical fluxes (e.g. Burd, 2024) and fundamental questions of ecosystem structure
18 (e.g. Woodson et al., 2018) and biodiversity (e.g. O’Dor et al., 2009) to more societal issues such as fisheries management
19 (e.g. Karp et al., 2023) and climate modelling (Kwiatkowski et al., 2020). However, the seafloor, or benthic, ecosystem has
20 received much less attention, particularly in the deeper regions away from the continental shelves. This is despite the regions
21 deeper than 1000 m constituting over half of the earth’s surface area (Ramirez-Llodra et al., 2010; Harris et al., 2014).

22
23 The benthic ecosystem of the deep ocean (aside from hydrothermal vents) is almost entirely dependent on external input for
24 food, with the majority in the form of organic material sinking down from the waters above. This means that the benthic
25 ecosystem is susceptible to changes in production of this organic material that may occur several kilometres above it (Ruhl et
26 al., 2008), such as in response to climate change (Yool et al., 2017). Benthic ecosystems are also subject to direct pressures
27 such as trawling, dredging, oil and gas activities, and seabed mining. To understand and to predict the future for benthic
28 ecosystems we therefore need models that adequately capture their response to such drivers, across the full ecosystem and over
29 appropriate timescales.

30
31 Building models that capture the key interactions within an ecosystem is of value for three reasons: construction of a model
32 forces us to identify the key processes and to articulate our understanding of them in a precise manner; the behaviour of the
33 model allows us to identify gaps and uncertainties in that knowledge; and by linking the model to forecasts for how
34 environmental drivers may change it allows us to make predictions for the fate of the ecosystem ~~based~~ across different
35 scenarios. One modelling strategy is to represent an ecosystem as different functional groups, particularly those linked to
36 particular fluxes of interest into and out of the sediment e.g. deposit feeders and aerobic/anaerobic bacteria (e.g. Butenschön
37 et al., 2016; Erntsen et al., 2018). This approach is valuable, for example, in [studying the biogeochemistry of](#) shelf systems
38 where the interactions between sediment, overlying water and benthic ecosystem may need to be captured because the feedback
39 on the overlying water column may be significant given the shallow depths. Shelf systems also benefit from a greater array of

40 data to constrain a model as they are more accessible for sampling than deeper waters. More generally, a paucity of data to
41 constrain a model or limited understanding of causal relationships are common hindrances, particularly for deep-sea
42 ecosystems because of the remote and challenging nature of the environment being studied. For situations where the ecosystem
43 can be approximated as unchanging in time, statistical methods have been used (e.g. Reiss et al., 2014), particularly for
44 modelling distributions of groups or individual species, but also for distributions of biomass (Wei et al., 2010; Jones et al.,
45 2014). For deep-sea ecosystems where data are sparser, an inverse approach has been used to estimate fluxes between
46 functional and size category components of the ecosystem at equilibrium (Soetaert & van Oevelen, 2009 ; Durden et al. 2017;
47 de Jonge et al., 2020), with the size classes mirroring those represented by typical benthic sampling techniques. However,
48 behaviour such as switch-feeding (e.g. alternating between suspension feeding and predation) in deep-sea fauna (Durden et al.
49 2015; Iken et al. 2001) complicates the use of discrete functional groups based on feeding types (Durden et al. 2017).

50

51 Another approach, is to represent the community purely as a collection of different size classes of organisms (Kelly-Gerreyn
52 et al., 2014; Blanchard et al., 2011; Laguionie Marchais et al., 2020) rather than as functional groups or species. As described
53 below, this offers considerable simplification in model structure and ~~paramaterisation~~parameterisation. Furthermore, by using
54 allometric relations to base the model on the ~~representation~~representation of rates, rather than stocks, this approach also allows
55 the response of ecosystems with time to be tracked.

56

57 Considerable attention has been given to observations showing relationships which appear to scale in a consistent way with
58 body size, both at a population (e.g. abundance - White et al 2007) and an individual (e.g. physiological rates - Gillooly et al.
59 2001) level. This phenomenon has been widely observed, on land (e.g. Nagy 1987), in the air (e.g. Niven and Scharlemann,
60 2005) and in the sea (e.g. Molony and Field 1989) including the deep ocean (Durden et al. 2019; McClain et al. 2012; Mahaut
61 et al. 1995). That such behaviour has been observed across many habitats and orders of magnitude in size of organism
62 unsurprisingly led to a search for a “Universal” law explaining such behaviour. Metabolic rate controls ecological processes
63 at individual and ecosystem levels by determining resource uptake and allocation. The Metabolic Theory of Ecology (MTE;
64 West et al., 1997; Brown et al., 2004) asserts that, to first order, this rate is controlled by the size of organism and the ambient
65 temperature. This provides a potential explanation for the existence of a ~~power-law~~power-law relationship between
66 physiological rates and body size. However, there remains a discussion over the taxonomic or functional scale at which other
67 features or processes might disrupt any universal scaling (Seibel and Drazen, 2007), the precise value of the scaling (Isaac and
68 Carbone 2010, Brey 2010; Glazier, 2022) and the extent to which such an approach applies to systems that are not in
69 equilibrium (McCarthy et al., 2019).

70

71 Notwithstanding these caveats, an allometric approach still has considerable value when applied at broad ecosystem scales.
72 To support use of an allometric approach, we give just a few examples for three key processes: growth, respiration and
73 mortality. Motivated by predictions of MTE, Ernest et al. (2003) successfully tested the predicted scaling exponent of -0.25
74 for growth rate, for organisms spanning 10^{-14} - 10^8 g in size. More specific to this study, with a focus on macrobenthos, Cusson
75 & Bourget (2005) brought together empirical relations from previous studies (their Table 8) that demonstrate similar evidence
76 of scaling of growth rate with size. For respiration, Mahaut et al. (1995) found a power-law scaling with size for deep-sea
77 organisms, spanning seven orders of magnitude. This was for a single location, however, so not suitable for testing a
78 temperature dependence. For mortality, McCoy and Gillooly (2008, 2009) brought together estimates of natural mortality
79 spanning 22 orders of magnitude including plants, fish, birds, mammals and invertebrates, finding that a ~~power-~~power-law scaling
80 with size plus an exponential dependence on temperature captures the dominant pattern. A restriction of their data purely to
81 invertebrates found a similar result (McCoy and Gillooly, 2009), still spanning 11 orders of magnitude in size. Again, focussed
82 on marine benthic organisms, McClain et al., (2012) analysed data for growth, respiration and turnover (which can be a proxy

83 for mortality) and demonstrated a clear power-law scaling with size, with additional support for an exponential relationship
84 with temperature. There are, therefore, reasonable grounds for adopting an allometric approach.

85

86 Kelly-Gerreyn et al. (2014) constructed a dynamic model for benthic organisms based on allometry such that physiological
87 rates vary with body size (Benthic Organisms Resolved in Size – hereafter “BORIS-1”). BORIS-1 was capable of reproducing
88 the size distribution of organisms at three sites contrasting in depth between 150m and 1600m. This model assumed that all
89 organisms were detritivores, eating from a common pool of detritus supplied by organic material sinking to the seafloor, the
90 particulate organic carbon (POC) flux. BORIS-1 demonstrated that an allometric model with a small number of physiological
91 processes (ingestion, assimilation and respiration/mortality) that are common to all organisms but scale with body size can
92 capture the size-distribution of biomass seen in observations. However, the model has several limitations. The first is that it
93 only represents a limited range of sizes (8.9×10^{-7} to 2.9×10^{-2} g wet weight). It was therefore necessary to assume a specific
94 fraction of POC flux that was consumed and respired by organisms not represented by the model, and hence not available to
95 the modelled organisms. The omitted organisms included both smallest (e.g. bacteria) and largest (e.g. large sea cucumbers)
96 size ranges. The physiological rates were also not dependent on temperature even though there is evidence that physiological
97 rates typically increase as the environment warms (e.g. Gillooly et al., 2001). ~~Additionally, t~~The mortality rate ~~also~~ had a
98 dependency on the POC flux in BORIS-1. This resulted in estimates of longevity that unrealistically varied across several
99 orders of magnitude for the same organism at different locations.

100

101 This paper presents an expanded and updated version of BORIS-1 that addresses these limitations. The resulting model,
102 BORIS-2, spans the full range of organism sizes, includes the physiological role of temperature, and is parameterised using a
103 larger dataset that includes observations from a greater range of sites with contrasting environments conditions, including the
104 abyssal ocean. A single parameter set that allows the model to capture the ecosystem structure across these sites is given and
105 examples are demonstrated for how the model may be used to study both local and global questions. It is worth stressing that
106 the aim of BORIS-2 is to capture broad ecosystem behaviour, i.e. macroecology, across the full range of body sizes, not to
107 capture the dynamics of specific species.

108 **2 BORIS-2 model description**

109 BORIS-2 represents benthic organisms spanning in size from bacteria to large metazoans (Figure 1). It does so by dividing
110 benthic organisms into size classes and using an allometric approach. The size classes are defined on the basis of individual
111 wet weight body mass (units grams wet weight – gwwt). From the smallest to the largest, each size class spans twice the range
112 of the former. More specifically, the mean body mass of organisms within a size class spans from 1.3×10^{-14} gwwt (13 fg) for
113 the smallest to 3.6×10^3 gwwt (3.6 kg) for the largest. The lower limit of the smallest class is 0.88×10^{-14} gwwt (9 fg) and the
114 upper limit of the largest is 5.1×10^3 gwwt (5.1 kg). The size classes are chosen to be consistent with those used for size-spectra
115 biomass data (e.g. Laguionie Marchais et al., 2020) and BORIS-1 (Kelly-Gerreyn et al., 2014). The smallest size class is based
116 on the smallest observed bacteria (Luef et al., 2015), using a conversion from gC to gwwt of 11.5 (Brey, 2010). The largest
117 size class is chosen to be broadly representative of benthic habitats. It is consistent with a detailed assessment of invertebrates
118 for a well-studied abyssal site, the Porcupine Abyssal Plain (one of the sites described in Section 2.4). These upper and lower
119 biomass limits, together with the factor of two scaling used between biomass size classes, sets the number of model size classes
120 to 59. For application of BORIS-2 to specific locations where larger organisms are known, the upper size limit is easily
121 changed. The BORIS-2 size range currently spans over 18 orders of magnitude.

122 2.1 Ecological interactions

123 BORIS-2 comprises a set of differential equations describing the time-varying behaviour of $N=59$ size classes ingesting a
 124 common resource, R , that represents the stock of detrital food available to the benthic community (i.e., in / on the seafloor or
 125 in the benthic boundary layer). The model does not capture any direct predation or cannibalism, and instead represents a
 126 community of detritivorous heterotrophs. This decision is based on the different nature of benthic and pelagic ecosystems.
 127 Total biomass in a size range increases with body mass in benthic ecosystems (e.g. Benoist, 2020; Kelly-Gerreyn et al., 2014).
 128 In the pelagic ocean, biomass is roughly equal across different sizes (Hatton et al., 2021). The greater accumulation of biomass
 129 in larger organisms in the benthic system is consistent with a greater transfer efficiency arising from a reduced role of predation
 130 and a greater role of feeding from a common detrital resource. We effectively assume that the dominant influence on benthic
 131 ecosystems is having neighbours competing for your food, rather than eating you. This assumption is discussed in more detail
 132 in Section 4.1.

134 The total biomass represented by all organisms per square metre in each size class i of nominate mass M_i (units: grams wet
 135 weight - gwwt) is represented as B_i (units: gwwt/m²) which varies with time, t (units: d), according to the equation

$$136 \frac{dB_i}{dt} = \overbrace{g_i \cdot f(R, B_i) \cdot B_i}^{\text{gross growth}} - \overbrace{r_i \cdot B_i}^{\text{respiration}} - \overbrace{m_i \cdot B_i}^{\text{mortality}} \quad (1)$$

137 where g_i is the maximum specific growth rate and r_i and m_i are the specific rates of respiration and mortality, respectively.
 138 All of g_i , r_i and m_i have units of 1/d. The function $f(R, B_i)$ represents how growth is limited by increasing population size
 139 and/or decreasing resource availability (see Section 2.2). The associated equation controlling the amount of resource, R (units:
 140 gwwt/m²), is

$$141 \frac{dR}{dt} = F - \sum_{i=1}^N \left[\overbrace{g_i \cdot f(R, B_i) \cdot B_i}^{\text{gross growth}} - \overbrace{m_i \cdot B_i}^{\text{mortality}} \right] \quad (2)$$

142 where F is the POC flux to the seafloor through gravitational sinking of detritus (gwwt/m²/d). Note that at equilibrium the rate
 143 of supply of organic material, F , equals the respiration by the whole ecosystem, $\sum_{i=1}^N r_i \cdot B_i$. It is assumed that the long-term
 144 burial of organic material in sediment is negligible compared to POC and total respiration fluxes. (Section 4.1 discusses how
 145 this assumption might be relaxed.) A linear mortality term, $m_i \cdot B_i$, is used in BORIS-2. (The reason for using this rather than
 146 the quadratic $\mu_i \cdot B_i^2$ parameterisation used in BORIS-1 is given in the Appendix).

147 2.2 Growth limitation: food scarcity and interference

148 The resource-growth limitation function, $f(R, B_i)$, reflects the impact on growth arising from competition for limited resources.
 149 This function is chosen to capture two effects. First, low availability of food, R , should lead to a reduced rate of intake and
 150 growth. Second, any increase in the number of organisms (for which B_i is a proxy) looking for food should reduce the likelihood
 151 of any individual finding it, a phenomenon known as interference (e.g. DeAngelis et al., 1975). More specifically, we assume
 152 the parameterisation

$$153 f(R, B_i) = 1/(1+a_i B_i/R) \quad (3)$$

154 The parameter a_i is present to account for how interference may scale with size. For example, larger organisms can search a
 155 given area more quickly than a smaller one, in general, either because motility generally increases with size or more simply
 156 because they occupy a greater area. Note that a_i is unitless. The function $f(R, B_i)$ varies between 0 and 1, with a value of zero
 157 entirely ceasing production-growth and a value of one leading to growth at the maximum rate, g_i . To demonstrate that the
 158 function has the required properties, first consider the case where R-food is very abundant such that ($R \gg a_i B_i$). Then $f(R, B_i)$
 159 ~ 1 and there is no limitation of growth. If resource is scarce such that $R < a_i B_i$, then $f(R, B_i) \sim R/(a_i B_i)$ which is always a value
 160 less than one but increases and decreases linearly with both resource, R , and abundance of organisms, represented by B_i . Note

161 that for simplicity we currently only incorporate competition for resources within a size class. This is the simplest assumption
 162 given that different size classes seek food at different spatial scales. What is a meal for a bacterium is unlikely to be a meal for
 163 a holothurian. It would, however, be straightforward to include competition from other size classes simply by using a sum over
 164 those classes in the denominator. The form of the interference parameter, a_i , is discussed in the next section (2.3). [Figure 2](#)
 165 [and Section 2.4 show further how the function \$f\(R, B_i\)\$ varies, in particular demonstrating that it affects all size classes equally](#)
 166 [i.e. that it does not lead to some size classes being food limited while others are growing near maximum rates.](#)

167 2.3 Allometric and temperature influences

168 In BORIS-2 allometry is used to describe four physiological or physiologically_-affected processes across the range of body
 169 sizes. The physiological processes are growth (g_i), respiration (m_i) and mortality (r_i). The physiologically affected process is
 170 growth limitation, controlled by parameter a_i . All of these are assumed to be determined by size (body mass) and environmental
 171 temperature.

172

173 The effect of temperature is assumed to be identical for all four processes and represented by a function, $\theta(T)$, which is taken
 174 to be

$$175 \theta(T) = \exp[-E \cdot \tau/k] \quad (4)$$

176 with

$$177 \tau = 1/(T+T_{abs}) - 1/(T_{ref}+T_{abs}) \quad (5)$$

178 where T is temperature (units: °C), T_{ref} (units: °C) is a reference temperature, $T_{abs} = 273.15$ K converts T and T_{ref} to units of
 179 Kelvin (K), and k is Boltzmann's constant (8.62×10^{-5} eV/K). This is a widely used formulation applied both in empirical studies
 180 (e.g. Brey, 2010) and papers developing ideas around the Metabolic Theory of Ecology (e.g. Gillooly et al. 2001). E (units:
 181 eV) is often described as an activation energy. We discuss the value chosen for E in Section 2.4.2. T_{ref} is chosen to be 20°C.
 182 While this may seem an arbitrary choice of reference temperature, it has no impact on rates. Using a different T_{ref} simply
 183 requires a numerical change in parameters (g_0 , r_0 , m_0 and a_0) to compensate for the change.

184 It is assumed that the three physiological rates (g_i , m_i and r_i) scale with body size in an identical way. ~~This is necessary as~~
 185 ~~otherwise it is not possible for the ecosystem to achieve steady state in all size classes simultaneously. A different scaling with~~
 186 ~~size for these processes would mean that even if growth, respiration and mortality balance for one size of organism, they would~~
 187 ~~not balance for others. This is purely taking the option requiring fewest assumptions given the current uncertainty in how these~~
 188 ~~rates vary with size.~~ As the link between interference and physiology is more tentative, a_i is [theoretically](#) allowed to scale
 189 independently [\(but see Section 2.5\)](#). More specifically, growth, respiration and mortality have common scaling exponent β ,
 190 whereas interference scales with exponent α :

$$191 g_i = \theta(T) \cdot g_0 \cdot M^\beta \quad (6)$$

$$192 r_i = \theta(T) \cdot r_0 \cdot M^\beta \quad (7)$$

$$193 m_i = \theta(T) \cdot m_0 \cdot M^\beta \quad (8)$$

$$194 a_i = \theta(T) \cdot a_0 \cdot M^\alpha \quad (9)$$

195 The values chosen for the [seven](#) parameters used in the model (g_0 , r_0 , m_0 , a_0 , α , β , E) are given in Section 2.5 (and Table 1),
 196 together with a description of the data used to constrain them. The performance of the model using this parameter set is then
 197 described in Section 2.6 and the uncertainties associated with their values are discussed in Section 2.7. Before then a steady

198 state solution for the model is presented, both for its own use and as a source of useful information for constraining parameter
 199 values.

200

201 2.4 Steady state solution

202 The model has a steady state solution which can be written in a simple form. This provides a means to initialise simulations,
 203 to validate dynamical model runs (if run to equilibrium) or to accelerate model runs where time-scales are longer than organism
 204 response times.

205 Indicating steady state values with an asterisk, the steady state solution is

$$206 R^* = \frac{F}{\sum_{i=1}^N \frac{r_i(g_i - r_i - m_i)}{a_i(r_i + m_i)}} \quad (10)$$

$$207 B_i^* = \frac{(g_i - r_i - m_i)}{a_i(r_i + m_i)} \cdot R^* \quad (11)$$

208 This steady state solution provides a few insights into the behaviour of the model. First, both resource, R , and biomass in all
 209 size classes, B_i , increase linearly with F . This is not surprising as we would expect abundance of detritus and biomass to
 210 increase with increasing food supply. Second, B_i scales with size with the same exponent, $-\alpha$, as $1/a_i$ (i.e. $B_i^* \propto M^{-\alpha}$). This is
 211 because g_i , r_i and m_i all scale the same with size, as mentioned above, and so the scaling of $(g_i - m_i - r_i)$ in the numerator for B_i^*
 212 is cancelled by the identical scaling of $(r_i + m_i)$ in the denominator. Hence, the biomass spectral slope is effectively set by
 213 interference. Although this might be unexpected it should be noted that the processes contributing to a_i are still very poorly
 214 known and its scaling is likely to be influenced by physiological processes, such as respiration associated with enhanced
 215 movement for example. The theoretical model of Damuth (2007) is potentially relevant here as it links competition for
 216 resources to allometric scaling and community wide energy use. Nevertheless, understanding the likely influences on
 217 interference is clearly a useful avenue for future research. A consequence of the inverse scaling of a_i and B_i^* is that $a_i B_i^*$ is
 218 the same for all size classes i.e. the growth limitation function f does not change with size at steady state.

219

220

221 Returning to the steady state solution, substituting Equations 6-9 into Equations 10 and 11 gives

$$222 B_i^* = \left(\frac{1}{r_0 \theta(T)} \right) \cdot \left(\frac{M_i^{-\alpha}}{\sum_{j=1}^N M_j^{\beta-\alpha}} \right) \cdot F \quad (12)$$

$$223 R^* = \left(\frac{a_0(r_0 + m_0)}{r_0(g_0 - r_0 - m_0)} \right) \cdot \left(\frac{1}{\sum_{j=1}^N M_j^{\beta-\alpha}} \right) \cdot F \quad (13)$$

224 In addition to showing explicitly that B_i scales as $-\alpha$, as already mentioned, Equation 12 also reveals that the steady state
 225 biomass is independent of growth and mortality except for the scaling (β) and temperature dependence ($\theta(T)$) that they share
 226 with respiration. While this might seem at first surprising, it is because of the fundamental constraint that total respiration must
 227 match the POC flux, F , of arriving new organic material, i.e. $F = \sum_{i=1}^N r_i \cdot B_i^*$. At equilibrium, any change in growth or
 228 mortality arising from changing either g_0 or m_0 , respectively, is compensated by a change in food resource (R), rather than in
 229 B_i , to maintain this balance. This balance is also reflected in the influence of r_0 in Equation 12, with an increase in it
 230 corresponding to a compensating decrease in B_i^* . Similarly, if the specific respiration rate increases as a result of temperature
 231 increase (see Equation 7) then the higher physiological overhead means that a lower B_i^* is maintained. Finally, it is worth
 232 noting that although the mass scaling of interference, α , influences B_i^* , a_0 does not.

233

234 The steady state solution is also of use in understanding the influence of interference in the growth limitation function. Equation
 235 11 implies that at steady state $a_i B_i^* = \delta R^*$ where

236
$$\delta = \frac{(g_i - r_i - m_i)}{(r_i + m_i)}$$

237 Because the physiological rates scale identically, and have the same temperature dependence,

238
$$\delta = \frac{(g_0 - r_0 - m_0)}{(r_0 + m_0)}$$

239 which is the same for all size classes and sites. (For the parameter set used here and described below, $\delta=1$.) Figure 2 shows
 240 how the interference function varies with both R and B_i , as they vary either side of their steady state values. Finally, it is worth
 241 noting that although the mass scaling of interference, α , influences B_i^* , α_0 does not.

242

243 **2.5 Observational constraints and choice of parameter values**

244 There are a range of observations that can be used to constrain parameter values but, as described below, none can be used to
 245 set a parameter value in isolation. Relationships between parameters must be used to link the different observations together
 246 as a collective constraint. As stated above, in choosing the remaining six parameter values it is necessary to link together
 247 constraints from different observations. Those constraints are described below (and visually summarised in Figure 3) but first
 248 it is worth statingIt is also worth noting that there is no objective way to use these multiple constraints. As will be seen below,
 249 the strength of some constraints is greater than others and trying to construct some overall cost function to optimise all
 250 parameters simultaneously would require considerable subjectivity in how the constraints were translated into costs and
 251 weighted relative to each other. For this reason, and because of the limited number of parameters and ability to calculate the
 252 outcome of a given parameter set extremely quickly, values have instead been chosen by trial and error for the seven parameters
 253 $g_0, r_0, m_0, \alpha_0, \alpha, \beta, E$ to give an acceptable, if potentially not optimal, fit to observations. A summary of values can be found
 254 in Table 1. While future users of BORIS-2 may choose to use a different approach to selecting parameter values, it will be
 255 seen in Section 2.6 that the current set does a reasonable job and Section 2.7 describes the consequences associated with
 256 adjusting these values.

257

258 ~~Only the mass scaling associated with interference, α , can be directly constrained individually from data. For the six other~~
 259 ~~parameters ($g_0, r_0, m_0, \alpha_0, \beta, E$) there is a range of different data that can provide constraints, but none directly match specific~~
 260 ~~parameters. Instead, relationships between parameters must be used to link the different bits of data together as a collective~~
 261 ~~constraint. Unfortunately, published empirical relationships cannot be used directly for growth, respiration and mortality in~~
 262 ~~BORIS-2. While previous studies have highlighted observational evidence for allometric relationships, they have either~~
 263 ~~focussed on either in just one physiological rate (e.g. Mahaut et al., 1995; Cusson & Bourget, 2005), or, in the case where they~~
 264 ~~have studied in several (e.g. McClain et al., (2012)), have not addressed the question of whether the relationships for different~~
 265 ~~rates are consistent i.e. whether they can balance simultaneously for organisms of different sizes. For a dynamic model (and~~
 266 ~~for real organisms and populations) this is essential and so. Because of the variations in scaling reported in these studies~~
 267 ~~(discussed in Section 2.7) we have used the observation of allometry as a starting point but allowed flexibility rather than~~
 268 ~~take a value for the scaling exponent from a specific study in details to allow the necessary balance to be achieved.~~

269

270 The following first describes the observational constraints. Based on these, the argument for the specific choices of parameter
 271 values is then given. ~~parameter choices and the data used to support them.~~ Table 1 has a summary of parameter values and
 272 Figures [23](#) and [34](#), and Table 2, summarise the observational constraints and associated model diagnostics used to select them.
 273 The code needed to generate Figures [23](#) and [34](#) is also available to allow the model to be re-tuned given additional data,
 274 different locations or different priorities (Martin et al., 2025).

275

276 ~~As stated above, only α , can be directly constrained. T~~Starting with the largest dataset, biomass can be used as a constraint for
277 ~~the interference parameter α .~~ The steady state solution (section 2.4) shows that ~~β_i~~ must scale in the opposite way to biomass
278 distributions. Suitable observations from five sites are ~~available used to in selecting-select~~ the value; a summary is found in
279 Table 2. The Clarion Clipperton Zone (CCZ) is a vast abyssal plain in the northeast Pacific. The data used here come from a
280 site (17.2° N 122.6° W) of depth 4150 m with a low temperature (1.5 °C). Fladden Ground (FG) is in a shelf sea (153 m) and,
281 unsurprisingly, with higher temperature (8 °C). The Faroe-Shetland Channel (FSC) is a connection between the North Atlantic
282 and the Arctic, with the lowest temperature (-1 °C) despite a depth of only 1623 m. The Oman Margin (OM) is a slope site
283 (507 m) and has the highest water temperature (13 °C). The final site is the Porcupine Abyssal Plain (PAP), which is the deepest
284 (4850 m), with reasonably cold temperature (2.6 °C). A general decrease of temperature with depth is overlain with
285 considerable variability due to local hydrography (notably FSC and OM). In addition to spanning a range of contrasting
286 temperatures and depths, the data from the five sites also covers complementary size ranges of organisms. CCZ data are based
287 on photographically surveyed megabenthos. FG, FSC, and OM data are based on physically sampled meio- to macrobenthos.
288 PAP is based on physically sampled macrobenthos and photographically surveyed megabenthos. For CCZ, the data can be
289 found in Benoist (2020), with sampling and methodology described in Simon-Lledó et al. (2019) and Benoist et al., (2019).
290 Details on data for FG, FSC and OM can be found in Kelly-Gerreyn et al. (2014). Additional information on the sampling and
291 laboratory methodology can be found in Kaariainen et al. (2006). The benthic ecosystem of the PAP site has been studied for
292 decades (Hartman et al., 2021). The data used here, and presented in Benoist (2020), combines analyses of macrobenthos and
293 megabenthos. Descriptions of observational approach and the analysis methodology for the megabenthos can be found in
294 Morris et al. (2016) and Durden et al. (2020b). For macrobenthos, this information can be found in Benoist (2020) and Ruhl
295 et al. (2023). Further details on the treatment of size-resolved data, e.g. to remove biases such as under-sampled size groups,
296 can be found in Edwards et al., (2017, 2020) and Ruhl et al. (2023). Observations of biomass versus size for each of the sites
297 are shown in Figure 32. These are referred to as biomass spectra and the gradient of the relationship (when plotted log-log as
298 here) as the spectral slope, or scaling exponent. Despite some variability, all sites exhibit an increase of biomass with body
299 size, and in a manner that is consistent with a ~~power-lawpower-law~~ relationship. Figure 32 also shows the exponents found by
300 fitting a ~~power-lawpower-law~~ to the observations from each site individually. ~~Note that values are given for α (the negative of~~
301 ~~the biomass scaling).~~ There is no strong relationship between fitted exponent and environmental parameters, though the smaller
302 magnitude scaling exponents for the two shallow sites is something that has previously been seen in physiological rates rather
303 than biomass (Mahaut et al., 1995). The OM site additionally has a low oxygen concentration (Demopoulos et al., 2003) which
304 has been suggested to have a disproportionate impact on larger organisms (Quiroga et al., 2005) and which could therefore be
305 responsible for flattening the slope relative to other sites. Nevertheless, here we take the simplest assumption that all sites are
306 showing sufficiently similar behaviour in scaling to assume a common scaling exponent across the sites, leaving an
307 investigation of departures from this for other studies. Figure 32g shows the simultaneous fit to data from all sites. It is seen
308 that observations from the five sites cover different size ranges such that the composite dataset spans a substantially wider size
309 range than any individual site. Furthermore, the relationship of biomass with size appears consistent across the wider range. If
310 the data from all sites is combined then the scaling exponent for a ~~power-lawpower-law~~ fit to all five sites simultaneously
311 indicates a ~~value for α of -scaling exponent of~~ 0.26 (s.d. 0.016, $r^2=0.76$, $p<0.001$). ~~Using The existence of similar scaling~~
312 ~~behaviour across~~ multiple sites ~~simultaneously~~ gives more confidence that the ~~parameter set presentedmodel~~ can be used
313 globally.

314

315 ~~As stated above, in choosing the remaining six parameter values it is necessary to link together constraints from different~~
316 ~~observations. Those constraints are described below (and visually summarised in Figure 3) but first it is worth stating that there~~
317 ~~is no objective way to use these multiple constraints. As will be seen below, the strength of some constraints is greater than~~
318 ~~others and trying to construct some overall cost function to optimise parameters would require considerable subjectivity in~~

319 ~~how the constraints were translated into costs and weighted relative to each other. For this reason, and because of the limited~~
320 ~~number of parameters and ability to calculate the outcome of a given parameter set extremely quickly, values have instead~~
321 ~~been chosen by trial and error for the six parameters $g_0, r_0, m_0, \alpha_0, \beta, E$. A summary of values can be found in Table 1. While~~
322 ~~future users of BORIS 2 may choose to use a different approach to selecting parameter values, it will be seen in Section 2.6~~
323 ~~that the current set does a reasonable job and Section 2.7 describes the consequences associated with adjusting these values.~~

324

325 ~~Perhaps the strongest~~The next observational constraint comes from the requirement that the supply of organic carbon to the
326 ecosystem (the POC flux, F) balances the total respiration of the organisms present at steady state. For the model, respiration
327 is given by the sum over size classes of the product of the specific respiration rate and biomass in each size class, $\sum r_i B_i$.
328 Therefore, observations of POC flux, co-located with the previously described size-resolved estimates of biomass, provide a
329 useful joint constraint on r_0 and β . There are several sources of data for POC flux. First, and most directly, for the PAP site
330 there is a long time-series of sediment trap data (Lampitt & Pebody, 2023). Although there are sediment traps at both 3000 m
331 and 4750 m, the latter is thought to be biased by sediment resuspension as it is just 100m above~~near to~~ the seafloor. The
332 magnitude of this effect can vary with time but previous work has shown that the flux near sea-bed at the PAP site is often in
333 excess of that at 3000 m due to re-suspension (Lampitt et al., 2000, 2001). For this reason, it is better to use-extrapolate the
334 estimate from the 3000 m trap. For the year 2012 (to best match the biomass observations) the annual carbon flux at 3000 m
335 is 1.91 gC/m²/yr. The associated flux at the seafloor can be roughly estimated using a widely used ~~power-law~~power-law scaling
336 (Martin et al., 1987), such that the flux at the seafloor at 4850 m equals 1.91 gC/m²/yr *(3000 m/4850 m)^{0.858} = 1.3 gC/m²/yr.
337 An alternative way to estimate the sinking flux at the seafloor is to use the Lutz et al. (2007) algorithm, which uses net primary
338 production, sea surface temperature and depth at a given location to estimate the flux. This allows estimates to be made for all
339 ~~five~~ sites (not just PAP) – see Table 2. Finally, Sediment Community Oxygen Consumption (SCOC) data (Stratmann et al.,
340 2019) also allows the sinking flux to be estimated, making the same assumption that the respiration (measured by oxygen
341 consumption) must balance this flux, in this case when averaged over the year. As SCOC is usually measured using chambers
342 of ~50 cm across, the estimates exclude or bias the contribution from larger organisms – not just those too large to fit but also
343 those too scarce to be robustly sampled in such an area - and care is needed in accounting for this (Laguionie Marchais et al.,
344 2020). More generally, all of these sources of POC flux data have significant associated uncertainties, which is why POC flux
345 was not fixed when deriving parameter values for the general use model configuration described here. Instead the model can
346 be used to estimate the POC flux and compared to these different observational estimates as a broader constraint. All
347 observational estimates of POC flux used to constrain model parameters, as well as the model values, are shown in Figure 43b.
348 These values are also given in Table 2. Note that even if there was no ~~scatter on~~uncertainty in the observations for POC flux
349 it would still not be able-possible to use the data to independently choose~~to~~ infer specific values for β and r_0 using the data.
350 This is because ~~it~~ is possible to simultaneously vary β and r_0 in a way that the total respiration remains unchanged. Note that
351 respiration also gives a link between the physiological (β) and interference (α) scaling exponents that needs to be considered.
352 Respiration by a size range of organisms is given by $r_i B_i$, which scales as $M_i^{\alpha\beta}$. Hence, the difference between α and β
353 determines whether the energy use by a size range increases ($\alpha > \beta$), decreases ($\alpha < \beta$) or remains with same ($\alpha = \beta$) with size.
354 We are unaware of observations indicating an increase with size but there are observations suggesting $\alpha = \beta$ (Laguionie
355 Marchais et al., 2020) and this is consistent with ‘energy equivalence’ which has been suggested theoretically (Damuth,
356 2007).~~Another constraint is needed.~~

357

358 The inherent relationships between the three physiological rates allow other observational constraints ~~to be found, for g_0, m_0~~
359 ~~and E , as well as for β and r_0 .~~ Observations indicating that physiological rates decrease with size were already described ~~in~~
360 Section 1. Additionally, the maximum net growth rate, g_i , must equal or exceed the sum of the respiration, r_i , and mortality,

361 m_i , for all sizes for ~~life-populations~~ to be sustainable. Together, these two statements imply that all rates must sit within a
362 'window' of parameter space (rate versus size, Figure 43c). ~~We therefore follow a similar approach to that of Mahaut et al.~~
363 ~~(1995) and Kelly-Gerreyn et al. (2014), by using constraints at smallest and largest sizes of organism. Having so many degrees~~
364 ~~of magnitude in size in the model means that care is needed for the parameter values to be realistic at the two extremes of the~~
365 ~~sizes reproduced. Using constraints at intermediate sizes risks significant under- or over-estimates for largest and smallest~~
366 ~~organisms through under-constrained extrapolation. Because rates are observed to decrease with size, the top left corner of~~
367 ~~the window is set by the upper limit for the specific growth rate of the smallest size class of organism. For benthic bacteria,~~
368 ~~we take a rough upper limit of 1/d maximum specific growth rate. Though Dixon and Turley (2001) find a rate of 0.1/d, a~~
369 ~~wide range reported by Giovannelli et al. (2013) includes a value of 6/d. An intermediate value of 1/d is marked in Figure 4c.~~
370 The bottom right corner of the window is set by the lower limit for the specific mortality or respiration rate (whichever is
371 smallest) of the largest size class. ~~The data collated by McClain et al. (2012) indicates lifetimes for the largest organisms (few~~
372 ~~kg wwt) of order 50 years. Given this and assuming the same scaling, β for all physiological rates as stated earlier. In practice,~~
373 ~~the comparison to POC fluxes described above indicates that respiration is a considerably larger rate than mortality, so~~
374 ~~mortality defines the bottom right corner of the 'window'. (Note that varying the scaling exponent β tilts the gradients of the~~
375 ~~lines in Figure 3e.) We therefore follow a similar approach to that of Mahaut et al. (1995) and Kelly Gerreyn et al. (2014), by~~
376 ~~using constraints at smallest and largest sizes of organism. Having so many degrees of magnitude in size in the model means~~
377 ~~that care is needed for the parameter values to be realistic at the two extremes of the sizes reproduced. Using constraints at~~
378 ~~intermediate sizes risks significant under- or over-estimates for largest and smallest organisms through under-constrained~~
379 ~~extrapolation. First, for benthic bacteria, we take a rough upper limit of 0.1/d maximum specific growth rate from Dixon and~~
380 ~~Turley (2001). This is marked in Figure 3e. As mentioned, this additionally constrains respiration and mortality whose~~
381 ~~combined sum must be lower than the maximum growth rate. Second, the data collated by McClain et al. (2012) indicates~~
382 ~~lifetimes for the largest organisms (few kg wwt) of order 50 years. This is also marked in Figure 43c and lifetimes for the~~
383 largest organisms at each site are also given in Figure 43e. Note that both of these constraints need to be treated a little flexibly
384 as it is not realistic to set a precise limit in either case.

385
386 There are two ~~further final, but more subjective~~ constraints, to ~~allow-inform~~ the choice of values for β , g_0 , r_0 , m_0 and E . First,
387 the ratio $(r_0+m_0)/g_0$ represents the fraction of the maximum growth rate, g_0 , achieved by organisms when the system is in
388 equilibrium. This should take a value less than 1 for food to be limiting, as is expected for the seafloor (Smith et al., 2008).
389 Second, decreasing E ~~brings the lines converges physiological rates~~ for the different sites ~~closer together~~, as the inter-site
390 differences due to temperature are diminished. Doing so ~~also~~ reduces the inter-site differences in model POC flux (~~and R~~) for
391 the same reason, because of the ~~need to match balance with~~ total respiration. ~~In summary, we take $\beta=0.1$, $g_0=0.017/d$,~~
392 ~~$r_0=0.015/d$, $m_0=0.0003/d$ and $E=0.35 eV$.~~

393
394 ~~The final observational constraint is Total Organic Carbon (TOC) in the benthic sediment which can be used to estimate the~~
395 ~~amount of detritus available as food, R , which itself is a constraint on~~ Once values for α , β , g_0 , r_0 , m_0 and E have been chosen,
396 ~~the remaining the~~ parameter to constrain is a_0 . This parameter influences the amount of detritus available as food, R , in the
397 ~~model~~. This can be seen in the steady state solution (Equation 13), where R increases linearly with a_0 . ~~To constrain a_0 , we~~
398 make use of the compilation of Parameswaran et al., (2024) who created an atlas of ~~Total Organic Carbon~~ TOC at the seafloor
399 surface, using a neural network approach applied to globally distributed estimates calculated over the top 10 cm of sediment.
400 This data source was chosen in preference to the alternative product of Atwood et al., (2020) as the latter used estimates over
401 the top 1m of sediment, which are an order of magnitude larger than those in Parameswaran et al., (2024) and likely to represent
402 carbon resources unavailable to the majority of detritivores on the seafloor. The estimates for ~~Total Organic Carbon (TOC)~~
403 using Parameswaran et al., (2024) for the five sites are shown in Figure 43cd. These are not directly comparable with R ,

404 however. There is considerable evidence that not all of sediment TOC is readily available as a food resource, with typically
405 5% (e.g. De Jonge et al., 2020; Van Oevelen et al., 2011a, 2011b) regarded as ‘labile’ i.e. easily consumed (see Discussion for
406 more on this). We therefore multiply our model estimates for R at the ~~five~~ sites by a factor of 20 to give an estimate of TOC
407 for comparison to the observational values. Estimates for TOC based on Parameswaran et al., (2024) are given in Figure ~~4~~
408 and Table 2, together with model estimates for R and TOC. There is considerable variability; in observations, model values
409 and their relative sizes. A weaker constraint for a_0 is the turnover time for R i.e. the time it would take for R to be replaced by
410 the POC flux (Figure ~~4~~d). A minimum turnover time of several years would be expected for the system to be able to achieve
411 steady state on an annual basis. ~~On the basis of these two constraints, a value of 500 is taken for a_0 .~~

412

413 ~~We now outline our choices of parameter values (Table 1) given the above constraints. Starting with α and β , taking $\alpha=\beta=-$
414 0.2 gives a scaling exponent consistent with observations for rates and energy equivalence but requires a biomass scaling that
415 is a little lower than the fit to observations. It is not possible to use the -0.26 scaling implied by the observed biomass spectra
416 without substantially worsening the fit between model and observational estimates of POC flux (Figure 4b). Given this scaling
417 for β , we take $g_0=0.001$ /d, $r_0=0.0045$ /d, $m_0=0.0005$ /d to fit rates within the window in Figure 4c. This also gives a value for
418 $(r_0+m_0)/g_0$ of 0.5, giving food limitation at steady state. We take a value of $E=0.35$ eV which is at the low end of observations
419 but using a larger value also worsens the match between model and observational estimates of POC flux. Finally, ~~On the basis~~
420 ~~of these two constraints, a value of 20~~500 is taken for a_0 as it gives the best agreement between model-estimated and observed
421 TOC (Table 2) across the sites given the other choices of parameter values.~~

422

423 ~~The sensitivity of key metrics to the model parameters is shown in Figure 5. For each metric, its fractional change for a +/-~~
424 ~~10% change in parameter value from the values given above is shown. This was carried out for each site assuming the observed~~
425 ~~temperature and the POC flux that is consistent with a model fit to the biomass observations with the imposed 0.2 scaling~~
426 ~~exponent. The three parameters, g_0 , α and β show the greatest sensitivity, with a 20-30% change for a 10% change in~~
427 ~~parameter. The exceptions are the largest organism lifetime, which is insensitive to g_0 and α , and total biomass, which is~~
428 ~~insensitive to g_0 . It should be noted that the sensitivities of α and β work in opposite directions, with a decreased metric for~~
429 ~~one corresponding to an increase in the same metric for the other. This means that any change to these parameters while~~
430 ~~retaining energy equivalence (i.e. $\alpha=\beta$) would have a reinforcing rather than a compensating effect. An obvious feature of the~~
431 ~~sensitivity analyses is that only E has an influence which varies across sites. This can be understood by looking at the steady~~
432 ~~state solution (Equations 10 and 11) and remembering that the temperature and POC flux are the only things that vary between~~
433 ~~sites as external influences. The sensitivity is calculated as the metric evaluated at the altered parameter value divided by the~~
434 ~~value at the standard value. For R , the POC flux cancels out in this calculation. The temperature effect (Equation 4) varies~~
435 ~~across sites, but R is already insensitive to this because growth, respiration, mortality and interference all share the same~~
436 ~~temperature dependence and their effects cancel each other out (Equation 10). As TOC is calculated simply as a constant~~
437 ~~multiple of R , it shares the lack of variation in sensitivity across sites. As the turnover time is calculated as the ratio of R to the~~
438 ~~POC flux (the latter of which cancels when calculating the metric, as described above), it also shows a sensitivity that is~~
439 ~~constant across sites. Two metrics do show variation in sensitivity across sites though. Equation 11 shows that the temperature~~
440 ~~effects do not cancel out for the biomass metric, so the sensitivity to E varies with temperature across the sites. Similarly, as~~
441 ~~the lifetime of the largest organisms is simply the reciprocal of their mortality, which varies with temperature across sites, it~~
442 ~~will too.~~

443

444 2.6 Model performance

445 ~~The parameter values chosen for the model, based on the above constraints, are shown in Table 1.~~ The observations at all ~~five~~
446 sites show a ~~power-law~~power-law distribution of biomass with size, and the model performs well in capturing this characteristic

447 at each site (Figure 32). Note that the matching of magnitudes in biomass for each size class across sites in Figure 32gf arises
448 from the normalisation for the simultaneous fit, not directly from model parameter value choices. Although the choice of E
449 influences the differences in biomass across sites, they are also influenced by inter-site differences in POC flux. For POC flux
450 (Figure 43b and Table 2), although there is some variability within the observations, the model and observational estimates
451 agree reasonably well and vary in a similar way across the sites. All have lowest fluxes at the deepest sites (CCZ, PAP), highest
452 at the shallowest (FG), and the fluxes at these two extremes differ by 1-2 orders of magnitude. For the physiological rates, in
453 Figure 43c the lines showing the rates should largely fall within 'window' marked by the two observational constraints marked
454 as dotted black lines, and described in Section 2.5. It is seen that although this is broadly the case, the chosen parameter values
455 already lead to this 'window' being stretched. Maximum bacterial (smallest size class) net growth rate is roughly 0.2 between
456 2-4 /d across the sites, a little higher than the reference value of 0.1 /d. The net growth rate achieved at equilibrium to first
457 order matches the respiration rate because mortality is so much smaller, and varies between 1-2 /d. Life expectancies for the
458 largest organisms are seen to span 29-6040-82 yr and straddle the reference value of 50 yr. Estimates for TOC using the model
459 vary from 5024 gC/m² to 2606400 gC/m². The observed range is smaller (from 320 to 2000 gC/m²) but given the large
460 variability in observation and model estimates across sites, the match is reasonable; at some places the model exceeds the
461 observed value and at others it is lower. The turnover time (Figure 43d) is seen to be estimated at ~20 yr, using either observed
462 or the model estimated POC flux. It is lower (3-15 yr) using the observations for POC flux (Figure 4b) and model estimate of
463 R because the model under-estimates the POC flux. Overall, using this set of parameters, the model does a reasonable job of
464 satisfying the constraints while simulating the biomass size distribution of the ecosystem at strongly contrasting locations.

465

466 2.7 Uncertainty in parameter values

467 Like any other ecosystem model, there is no single objective choice of parameter values here and it is always recommended
468 that sensitivity studies are done to ascertain the robustness of any conclusions drawn when using BORIS 2. The sensitivity
469 analysis shown in Figure 5 and discussed in Section 2.5 indicates the consequences of changing the current values.
470 However, Additionally, it is insightful to understand some of the restrictions on changing the values of the parameters.

471

472 The most tightly constrained parameter is α which, as described earlier, is inferred. A significant constraint arises from the mass
473 scaling exponent for the biomass observations at the different sites. If α the scaling exponent is estimated using data from just
474 a single site (Figure 32a-e), the estimates vary from -0.19 (for FG) to -0.33 (for CCZ). The uncertainty is largest at OM (CI: [-
475 0.13, -0.34]) and smallest at PAP (CI: [-0.248, -0.284]). If data from all sites are combined, as described in Section 2.5, then α
476 the exponent is estimated at -0.26. As the parameter set presented here is intended as one for general use, a
477 sensitivity analysis was done on how the estimate varies if data from each site in turn is excluded. Excluding data from CCZ,
478 FG, FSC, OM and PAP in turn gives an estimate for α that a value that varies between -0.25 and -0.27. Hence, none of the
479 individual sites is having a significant effect on the estimate of α the biomass scaling exponent. As described in Section 2.5,
480 the value used for the interference scaling exponent in the model is equivalent to having a biomass scaling exponent
481 of 0.2, below the values obtained from the observations described above. Also as described in Section 2.5, using a greater
482 magnitude value would either lead to a dominance of respiration by larger organisms (rather than the 'energy equivalence' for
483 which there is some observational support) or require an equivalent increase in the magnitude of the scaling
484 exponent for the physiological rates.

485

486

487 -The chosen value of -0.21 for the exponent, β , is at the lower end within the range of observational estimates. Most of these
488 cluster around -0.2 to -0.25 (e.g. Mahout et al., 1995; Ernest et al., 2003). Lower values have been found though. McCoy &
489 Gillooly (2009) reported an exponent of -0.18 for invertebrates. Lower still, McClain et al. (2012) found an exponent of -0.11

490 for growth of benthic organisms, though noted that this was inconsistent with the exponents they found for respiration and
491 mortality (-0.2 and -0.24 respectively). ~~However, looking at Figure 43c it is apparent that a using larger magnitude (perhaps~~
492 ~~to allow a biomass scaling of 0.25 and retain energy equivalence)~~ would lead to a lower average respiration rate across the size
493 classes, as the respiration rate for the smallest size organism cannot get any bigger. An increase in the magnitude of β would,
494 therefore, lead to a reduction in the model estimate of the POC flux and the quality of its fit to observations. For example, if β
495 were changed to -0.1825, then r_0 would need to be reduced by a factor of 105 to meet the constraint arising from the maximum
496 bacterial growth rate and the model POC flux estimates would ~~therefore also~~ decrease by a factor of 105, making them ~~at least~~
497 ~~aa further~~ factor of 5 lower than observations, ~~which the model already underestimates.~~

498
499 The value chosen for E (0.35 eV) is ~~also~~ at the lower end of values derived from observations. For a range of organisms not
500 restricted to marine ones, Savage et al. (2004) found ~~a range of~~ values from 0.35eV to 0.84 eV. McClain et al. (2012) estimated
501 E as 0.47eV for respiration and mortality but, with less confidence, 0.16 eV for growth. McCoy & Gillooly (2009) found a
502 value of 0.69 eV for respiration. For comparison, the canonical value for MTE is 0.63 eV (West et al., 1997; Brown et al.
503 2004). The greatest influence of E is in accounting for significant differences in physiological rates between sites with strongly
504 contrasting temperatures. Changing temperature from 0°C to 10°C with $E=0.35$ eV increases rates by a factor of 1.78. Using
505 $E=0.4563$ eV increases rates by a factor of 2.6. ~~To illustrate the impact of such a change~~ ~~However, the POC fluxes at PAP and~~
506 ~~CCZ—the two sites where the model flux is lower than all observations—decrease by ~20% if $E=0.6345$ eV, worsening the~~
507 ~~fit to observations then model-estimated POC fluxes reduce by 24-57% across the sites. This is because the temperature effect~~
508 ~~(T) takes lower values with the larger E even though the difference between (T) at different temperatures is greater.~~

509
510 The greatest subjectivity in choice of parameter value is in deciding the ratio $(r_0+m_0)/g_0$ which represents the fraction of the
511 maximum growth rate that an organism achieves at equilibrium. Another perspective on this is that it represents the degree of
512 food-limitation, with a value of 0 representative of total starvation and a value of 1 of a surfeit. We subjectively took this ratio
513 to be 0.95, ~~such that it is to be consistent with~~ a food-limited ecosystem. ~~It might be felt that this is not indicative of strong~~
514 ~~limitation, which might otherwise be expected in an ecosystem which is~~ dependent on material that is already the meagre
515 remains of food that was available to many other organisms as it sank down through the water column (Smith et al., 2008).
516 ~~However, because of the bacterial growth rate limitation, reducing this ratio further would lead to reductions in POC flux~~
517 ~~estimates.~~ It should also be appreciated that two locations with high and low food supplies do not necessarily differ in the
518 degree of food limitation, as the population sizes at the two sites will reflect the supplies. ~~It is unlikely that direct observations~~
519 ~~will become available to constrain this ratio so changes to the current value are more likely to arise from a wish to change one~~
520 ~~of the three component parameters, g_0 , r_0 or m_0 .~~ Keeping β fixed, the first two of these, g_0 and r_0 , are already at the upper
521 limit of observations whilst m_0 is at the lower limit (Figure 4c). Figure 5 shows that decreasing g_0 by 10% would lead to a
522 ~~~25% increase in R , TOC and turnover time. It would also increase the time for the perturbed system shown in Figure 7 to~~
523 ~~recover to 95% of the steady state value from 59 to 71 years. A 10% decrease in r_0 would result in the same decrease in~~
524 ~~estimated POC flux (or a compensating 10% increase in total biomass if it was wanted to preserve the total respiration, Figure~~
525 ~~5). The same 10% decrease in r_0 would give a ~10% decrease in R , TOC and turnover time (Figure 5). Finally a 10% increase~~
526 ~~in m_0 would give a 10% decrease in lifetime for the largest organism. Returning to the ratio $(r_0+m_0)/g_0$, a 10% decrease in r_0~~
527 ~~and m_0 would give a 10% decrease in the ratio $(r_0+m_0)/g_0$ to 0.45. Decreasing g_0 by 10% would increase it by 11% to 0.56.~~

528
529
530 ~~Although the parameter a_0 effectively controls the amount of detrital food, R , at steady state, changing it does not affect the~~
531 ~~degree of growth limitation.~~ A change in a_0 results in a compensating change in R (Equation 11 shows that they are proportional
532 at steady state) and consequently for the model estimate for TOC. The current value of a_0 was chosen ~~to minimise~~

533 $\sum_{\text{sites}} [\log(\text{TOC}_{\text{est}}/\text{TOC}_{\text{obs}})]^2$. Obviously, the choice of a_0 is sensitive to the subjective choice of this function. If a simple sum
534 of squared differences was used instead then a choice of $a_0 = 500$ would be more optimal, giving a lower range of estimates
535 than those given in Figure 4e and Table 2 (9.2 gC/m² CCZ; 2400 gC/m² FG; 560 gC/m² FSC; 960 gC/m² OM; 74 gC/m² PAP).
536 We used the logged ratio to choose a_0 here because of the orders of magnitude difference between observations across the
537 sites (Figure 4e, Table 2). Using a simple sum of squared differences biases the value to best fit observations with largest TOC
538 concentrations, such that the ratio a_i/R in the growth limitation term is unchanged. However, by influencing R , choosing a
539 different value for a_0 can affect the dynamics of the system when not in steady state. For example, it affects the turnover
540 time of R i.e. the time it takes the POC flux to replenish R if removed, has the same sensitivity to a_0 . This can affect the
541 recovery time to perturbations. Having slower recovery of R increases the recovery time for small organisms that would
542 otherwise recover much quicker than large ones because of higher physiological rates. The small organisms they cannot fully
543 recover until R itself is recovered. This is apparent in the example of how BORIS2 may be used to study a response to a change
544 in POC flux given later (Section 3.2 and red Figure 7). Using a value of $a_0 = 500$ in this example would reduce the time taken for
545 the total biomass to recover to 95% of the steady state value from 59 to 27 years. Reducing a_0 would lead to lower model
546 estimates of TOC (though admittedly there is considerable variability in observations) and a faster turnover for R . Turnover
547 times estimated using the model are also affected by choice of a_0 as shown in Figure 53d. They are consistently ~20 years for
548 the current choice of a_0 but reduce to 5 years if $a_0 = 500$. For the ecosystem to be in steady state on timescales of a
549 year, the turnover times need to remain significantly larger than one year.

550

551 3. Use of BORIS-2

552 BORIS-2 runs easily and quickly in Matlab (it was developed, tested and run in version [25.1.0.2973910 \(R2025a\) Update](#)
553 [19.12.0.2009381 \(R2022a\) Update 4](#)), and a steady state solution (Section 2.4) is available for situations where equilibrium is
554 the focus. The model requires only the seafloor temperature and POC flux for a location as inputs. If BORIS-2 is to be used at
555 a specific location then it may be possible to estimate the local POC flux directly using in situ data from sediment traps (e.g.
556 Durden et al. 2020a; Smith et al., 2013), although the resuspension of material means that near seafloor data should be treated
557 with care. Alternatively, if it is intended to use BORIS-2 over larger areas, such as basin scales, then POC flux can be estimated
558 less directly using algorithms which estimate POC flux at any given depth using satellite remote sensing data (Lutz et al.,
559 2007) or using global biogeochemical model output (e.g. Yool et al., 2017; Figure 3.21 of Cooley et al., 2022). Alternatively,
560 observations of sediment community oxygen consumption (SCOC) rates (Smith et al., 2013; Stratmann et al., 2019), which
561 would be expected to roughly balance POC input on timescales for which the system could be viewed as in steady state, could
562 be used. We now give a few examples to illustrate the range of potential uses.

563

564 3.1 Using the steady state solution

565 If it is of interest to know how benthic biomass (i.e. the total amount of organisms that can be sustained) varies geographically,
566 it is useful to focus on the annual average biomass such that it can be assumed that the ecosystem is in steady state to first
567 order. This assumption allows Equations 10 and 11 to be used for quicker calculations. In Figure 64, use is made of data for
568 POC flux and temperature at the seafloor to produce a global map of benthic biomass. The POC flux data are generated using
569 the Lutz et al. (2007) algorithm while seafloor temperature data come from the World Ocean Atlas (Reagan et al., 2024).
570 Temperature is largely uniform, with little change across the abyssal plains, or even above seafloor ridges, due to the weak
571 vertical gradients in temperature in the deep ocean. The pattern of low values in subtropics with higher values in tropical,
572 subpolar, polar and coastal regions for the POC flux is similar to that seen in the export of organic material from the ocean
573 surface (e.g. Nowicki et al., 2022) but superimposed on this is the effect of depth. POC flux attenuates strongly with depth
574 (Martin et al., 1987), and a logarithmic scale is needed to capture the variation in seafloor POC flux from shelf to abyssal
575 regions. Because of the largely uniform distribution of seafloor temperature, that of seafloor biomass closely resembles that of

576 the POC flux for much of the ocean. Only in the Mediterranean and Red Sea are the impacts of much higher temperatures
577 visible as-with lower biomasses relative to the variations in POC fluxes because they need to balance greater physiological
578 rates.

579

580 3.2 Running the model dynamically

581 The dynamic version of BORIS-2 runs easily on a standard laptop, taking just seconds for a thousand years. The forcing data
582 on POC flux, F , and the temperature, T , can also both vary with time if required. This allows a variety of transient responses
583 to be explored.

584

585 For temperature, long-term temporal change in deep-water temperatures has been detected, but is of a very small magnitude
586 (e.g., <0.002 °C/yr Garry et al., 2019). Stronger fluctuations at a site may arise near the boundaries of warm (e.g. Red Sea,
587 Mediterranean Sea), cool (e.g. Atlantic, Pacific, Indian Oceans), or cold (e.g. Arctic and Southern Oceans) deep waters if their
588 boundaries move in response to natural or climate-change related shifts. For example, at the Arctic-Atlantic transition in the
589 Greenland-Iceland-Faroe-Shetland region a 10°C shift in bottom water temperature can occur over a short spatial (bathymetric)
590 scale (e.g., Turrell et al., 1999) and so a near 10°C shift can occur on short time scales (hours, e.g., Bett, 2001). Generally,
591 though, because a 10°C change in temperature is required to create a roughly factor of 2 change in physiological rates, scenarios
592 where time-varying temperature has a significant impact on biomass are likely to be rare for deeper, off-shelf locations.

593

594 Significant changes in POC flux are more likely. For example, considerable uncertainty remains over the impact of climate
595 change on export of organic carbon from the ocean surface but future changes of up to 41% are possible (Henson et al., 2022).
596 Such changes in POC flux leaving the surface will impact the benthic ecosystem, which is dependent on the fraction of this
597 export that reaches the seafloor. One application of the dynamic version of BORIS-2 therefore is in exploring climate change
598 consequences for the benthos (e.g. Yool et al., 2017). A much simpler example of how the model can be used, to study
599 responses to change in POC flux is shown in Figure 75. Here the ecosystem is initially in steady state but then the POC flux is
600 doubled. As is apparent in Figure 32, the different sizes of organisms will have very different biomasses. Hence, for ease of
601 comparison the biomasses and detritus are normalised in Figure 7 by dividing by their final value. Similarly, the variation of
602 physiological rates with size means that response times differ with size of organism. Using a log time scale allows this to be
603 seen more clearly. The smallest size class tracks the response of the detritus closely because faster physiological rates allow
604 these organisms to respond as quickly as the detritus changes. The larger organisms have slower rates and are seen to respond
605 significantly more slowly as a consequence.

606 4 Discussion

607 The BORIS-2 model has been presented. It allows simulations of the benthic community across the full size-range of
608 organisms. A single parameter set has been provided for general use as-it-that allows the model to reproduce observed biomass
609 size distributions at five sites contrasting strongly in location, depth and temperature, while meeting other constraints on POC
610 flux, expected physiological limitations of smallest and largest organisms and the amount of organic carbon available for food
611 on the seafloor. It is intended that BORIS-2 be used in a macroecological manner, not to represent the dynamics of specific
612 species. Physiological processes for organisms within the same size class can vary significantly so BORIS-2 is best suited for
613 examining questions related to the overall community or the relative behaviour between size classes. As with any model there
614 are aspects that represent limitations and, as a result, areas for further investigation.

615 4.1 Model assumptions

616 BORIS-2 assumes all organisms are detritivores feeding from the same common resource, detrital organic carbon on the
617 seafloor. In practice, a community will have organisms exhibiting a variety of feeding strategies of which detritivory is just
618 one. Predation, for example, is not captured explicitly by BORIS-2. However, on seafloors deeper than the euphotic zone and
619 outside of chemosynthetic systems, the benthic ecosystem is supported solely by the POC flux and predation is effectively a
620 secondary transformation of that carbon. One interpretation is that BORIS implicitly captures predation in the mortality term
621 but that the gains are distributed across all size ranges rather than received by specific ones. Even from that perspective,
622 BORIS-2 may under-estimate predation because mortality is parameterised based on natural mortality rate data. In the absence
623 of suitable data for predation rates and given the large uncertainties in natural mortality, the magnitude and significance of this
624 underestimate are uncertain. Separate population dynamics for detritivore and predator components of the benthic community
625 have been studied on the shelf (Blanchard et al., 2009) where it was found that predators might display a stronger increase of
626 biomass with size than detritivores. A size-based model presented in the same work to explore this interaction further found
627 that the presence of predators could cause a steepening of the biomass spectrum for detritivores where their size overlapped
628 with the prey range for predators. However, the predators of benthic organisms were assumed to be largely pelagic – a condition
629 that is not experienced in the deep ocean. While a similar coupled approach could be adopted in BORIS-2, the main difficulty
630 in incorporating carnivory into BORIS-2 is the requirement for data on the relative abundance of predators versus non-
631 predators across size classes. Such data are scarce even on the shelf (e.g. Blanchard et al., 2009). Without such information it
632 would be difficult to constrain sufficiently the model parameters.

633

634 An additional facet of the ecosystem that is simplified by BORIS-2 is how the organisms obtain their food. In reality, they
635 may be more or less mobile, allowing them to search for food. They may also be able to filter organic matter from seawater as
636 suspension feeders, intercepting food before it hits the seafloor or exploiting resuspended or advected material. In theory, the
637 parameter a_0 could be modified to reflect greater mobility while the growth parameter, g_0 , could be adjusted to capture the
638 effect of suspension feeding. Once again though, to incorporate such changes would require additional data on the relative
639 abundance of organisms with these different characteristics across size ranges.

640

641 A final assumption of BORIS-2 worth discussing is that no organic material is either refractory or buried. For burial, a fraction
642 of the POC flux and/or the mortality could alternatively be regarded as buried and removed from the system. Note that the
643 POC flux would then have to balance the sum of burial and respiration, so a lower respiration would be required to balance
644 the same POC flux. ~~However, estimates for burial vary from 37% of the POC flux arriving at the seafloor on the shelf to 4%
645 in the deep (>2000m) oceans suggest that at most 10% of the POC flux would be buried (Dunne et al., 2007). The shelf value is
646 in the absence of perturbations to the sediment such as fishing related trawling. Based on the low deep-sea fraction, burial is
647 omitted, so adding this process is unlikely to have significant effects on model dynamics or parameter values. For this reason,
648 it is omitted. It could easily be added as a (depth-dependent) 'tax' on seafloor POC flux if needed subsequently.~~ Regarding
649 refractory organic carbon, it was described in Section 2.4 that it has been assumed that only 5% of the total organic carbon in
650 the surface sediment is readily available to the benthic ecosystem represented by the model. The other 95% is regarded as
651 refractory. Consider two scenarios. The first is that the POC flux arriving at the seafloor is entirely labile and refractory carbon
652 is created only by the seafloor ecosystem. In this case, it would be possible to modify BORIS-2 such that a fraction of mortality
653 passed into a refractory carbon pool rather than into R . In the second scenario, the POC flux has a refractory component. This
654 could be directed straight into a refractory pool. Reality is likely to be some combination of these two scenarios. At steady
655 state, all of the organic carbon entering the refractory pool must either be respired or transformed to labile material and hence
656 returned to R . In the hypothetical case of no respiration, then the flux of organic material into and out of the refractory pool
657 should balance, such that the net flux is zero. This is the implicit assumption in BORIS2, such that this exchange is not
658 modelled. In reality, some of the refractory carbon will be respired, and this could be incorporated in BORIS-2 in the same

659 way as burial, as a simple extra loss; applied to the POC flux or by adding creation and respiration of refractory material by
660 the benthic community as appropriate. In the absence of data from multiple sites for the amount of refractory carbon arriving
661 as POC flux or created by the benthic ecosystem, and the fraction of this that is eventually respired or buried, the dynamics of
662 the refractory pool are omitted. An additional aspect of the refractory carbon dynamics is that there will be a bacterial
663 population carrying out itsthe respiration that is also not captured by BORIS-2. This means that observational estimates of
664 bacterial abundance in seafloor sediments are likely to be higher than those predicted by BORIS-2. With a large pool of
665 refractory carbon (Section 2.54) and associated bacterial doubling time up to thousands of years (Jørgensen & Marshall, 2016),
666 this additional population is likely to be much larger than represented by the smaller size classes of the model that are feeding
667 on *R*. For example, bringing together observations from a site in the abyssal Pacific to apply a linear inverse model for the
668 benthic system including refractory carbon, de Jonge et al. (2020) estimated the prokaryotic biomass to be roughly equivalent
669 to that for megafauna. In BORIS-2, the biomasses for the equivalent (smallest and largest) size classes differ by a factor of
670 10^5 . This is not a straightforward comparison though as the prokaryotes in the de Jonge (2020) study feed from both labile and
671 refractory material. If future data suggest that bacteria need to be taken out of the allometric framework and treated separately,
672 the biomass estimates of remaining organisms are unlikely to change by more than a factor of two (the extreme case of bacteria
673 having total biomass equal to all other organisms present), with relative biomass of other classes unchanged. To make such a
674 change though would require information on the flux or fraction of organic carbon entering the refractory pool, and the
675 physiological rates of the bacteria ingesting and respiring it. Note that the very definition of “refractory” is itself an uncertainty.
676 The wide flexibility in the structure of molecules of organic carbon means that POC varies widely in how “labile” or
677 “refractory” it is. It is not a simple binary, so this adds a further layer of uncertainty.

678
679 Nevertheless, treating bacteria differently could offer one means of increasing the total respiration to give an improved match
680 to the observations for POC flux and oxygen consumption (Figure 4b). As an extreme example, if only bacteria were allowed
681 access to the POC flux arriving at the seafloor (rather than everything having equal access at present), with the detrital pool
682 being supplied instead by dying bacteria, then the observed biomass of other organisms would be supported by a fraction of
683 the POC flux equivalent to the ratio of mortality to respiration of the bacteria. This ratio is 0.1 for the current parameter set.
684 Without changing any parameter values this approach would therefore decrease the POC flux available for other organisms in
685 Figure 4b by an order of magnitude, with respiration of those organisms now exceeding estimates, as anticipated. It would also
686 increase bacterial biomass by two orders of magnitude (but still three orders of magnitude less than the total). Although there
687 is some evidence that bacteria respond quickly to POC deposition (Sweetman et al., 2018), other similar studies show a wider
688 response, including a rapid response by macrofaunal invertebrates (Witte et al., 2003). Note that the latter studies were
689 conducted at small physical scales that effectively exclude megafaunal invertebrates such that their relative influences and
690 responses are unknowns (Laguionie Marchais et al., 2020). Such an approachThe option to treat bacteria differently is therefore
691 left for future study.

692 4.2 Other possible model extensions

693 An aspect of BORIS-2 which may benefit future development is the restricted number of external influences. There are
694 currently only two: the supply of detrital material to the seafloor (POC flux) is the food source for all organisms and ambient
695 temperature is the only control other than size on metabolic rates.

696
697 The effect of oxygen concentration in seawater is not currently included in BORIS-2. Although it has been questioned whether
698 there is clear evidence for an oxygen effect on metabolism (Siebel and Drazen, 2007), a lack of clear response to low oxygen
699 by benthic communities might be as a result of a shift in community composition towards organisms more efficient at extracting
700 oxygen from waters with low concentrations (Childress and Seibel, 1998). That said, under reduced oxygen concentrations

701 there is evidence that macrobenthos shift to smaller body sizes (Pearson & Rosenberg, 1978), while meiobenthos may shift to
702 large body sizes (Moore & Bett, 1989). There may even be a tendency for megabenthos to be eliminated (Pearson & Rosenberg,
703 1978), though they may be enhanced at the peripheries of oxygen minimum zones (OMZs; Levin, 2003). Given the anticipated
704 expansion of oxygen minimum zones through climate change (Busecke et al., 2022), it is worth noting that commonly applied
705 thresholds for hypoxia range from 0.3-4 mgO₂/L, with a modal value of 2 mgO₂/L. However, the lethal and sublethal levels
706 for individual taxa vary greatly (Vaquer & Duarte, 2008). In a formal environmental monitoring context (e.g. EU Water
707 Framework Directive), oxygen concentrations below 4 mg O₂/L are considered to be of concern (Best et al., 2007). There is
708 therefore value in finding a way to incorporate an oxygen effect in BORIS-2 if sites <4 mgO₂/L are of interest, and particularly
709 if concentrations are likely to be below 2 mgO₂/L.

710

711 The impact of seafloor type is another area where BORIS-2 may benefit from further analysis and expansion. At present, for
712 simplicity, BORIS-2 makes no distinction in the nature of the seabed environment, other than bottom water temperature and
713 POC flux. The implicit assumption is that it is applied in a sedimentary environment. In practice, the seafloor represents a
714 range of environments varying on scales from a single manganese nodule to an ocean basin. Seafloor type can influence both
715 motility (with some suspension feeders favouring hard substrata) and the efficiency with which food can be obtained (such as
716 hills or trenches which can focus bottom currents carrying suspended POC). Whether BORIS-2 can be configured for different
717 seabed environments by suitably adjusting parameter values and/or by splitting the ecosystem into populations with different
718 feeding traits is left for future developers.

719 5 Conclusions

- 720 • Based on allometric scaling of metabolic processes, the BORIS-2 benthic ecosystem model is capable of simulating
721 population dynamics of organisms ranging in size from bacteria to large metazoans, over 18 orders of magnitude.
- 722 • The only external information required is the POC flux to the seafloor and the ambient temperature.
- 723 • It can be run dynamically but a steady state solution also exists and is given.
- 724 • A parameter set is provided suitable for general use globally and capable of simultaneously providing a good
725 reproduction of observed biomass size spectra at five locations contrasting in depth, food supply, and temperature,
726 ~~and oxygen concentration.~~
- 727 • This model offers considerable flexibility in application, at a range of scales, from responses to regional perturbations
728 such as deep-sea mining, to studies of climate-driven global change in the benthos.

729

730 Appendix: Differences between BORIS-1 and BORIS-2

731 A brief description is given here of the differences between the BORIS-1 and BORIS-2 models. Full details of BORIS-1 can
732 be found in Kelly-Gerreyn (2014).

733 (1) Range of organism sizes reproduced

734 BORIS-2 has been designed to reproduce the full range of benthic organism sizes, whereas BORIS-1 focussed on a
735 limited range of sizes coincident with the data then available for comparison. BORIS-2 overlaps exactly with the 16
736 size classes of BORIS-1. ~~S~~ size class 27 of BORIS-2 matches size class 1 of BORIS-1. BORIS-2 therefore extends
737 for 26 smaller size classes and 17 larger size classes than BORIS-1, to provide more complete coverage of the range
738 of organism sizes.

739 (2) Choice and representation of physiological/ecological processes

740 Broadly, BORIS-1 and BORIS-2 are structurally similar, with dynamics arising from the three processes of growth,
741 respiration and mortality - but they differ a little in how they do this. First, in BORIS-1 growth is the net effect of

742 ingestion then assimilation. Ingestion was allowed to scale with body size in BORIS-1, but assimilation was just
743 assumed to be a fixed fraction of this. The difference between them was treated as waste and returned to R . To simplify
744 this in BORIS-2, a single net growth rate is used, effectively the combined product of ingestion and assimilation.
745 Also, in BORIS-1, growth rate increased linearly with the amount of food available. In practice an organism's ability
746 to ingest and assimilate food cannot increase indefinitely. In BORIS-2 the representation of growth is therefore
747 modified such that it saturates at high food abundance. It is also modified to include the effect of other organisms
748 competing for the limited food supply (Section 2.2). Second, respiration in BORIS-1 is represented as a fraction of
749 growth, and this fraction can vary independently with size. A consequence is that BORIS-1 does not specifically
750 capture basal metabolism, the 'tax' paid by any organism just to keep alive. In BORIS-2 respiration is represented as
751 a separate process independent of growth. This better represents basal metabolism. Additionally, an organism will
752 need to fuel active metabolism, the energy requirements above basic maintenance required for such things as
753 movement. In BORIS-2 it is implicitly assumed that this is included in the net growth rate. In BORIS-1 it was also
754 necessary to assume a fixed fraction of POC flux that was respired by organisms not captured by the model. By
755 expanding the size range to cover all organisms in BORIS-2, this assumption (and parameter) is no longer required.
756 Third, a linear mortality parameterisation was used in BORIS-2, in place of the quadratic one used in BORIS-1. This
757 choice is influenced by the impact of the mortality term on organism lifetimes. Temperature has been argued to be
758 the first order control on mortality (e.g. McCoy and Gillooly, 2008). There is found to be roughly a factor of two
759 increase in mortality rate per 10°C increase in environmental temperature. As context, the sites described in Section
760 2.5, which span from shelf to deep ocean, only encompass a 14°C range of temperatures, roughly consistent with a
761 factor less than 4 range in mortalities. The quadratic parameterisation, however, leads to a dependence of the specific
762 rate of mortality on biomass (i.e. with a quadratic mortality term the specific rate is $\mu_i B_i$), and hence on food supply
763 (the POC flux, F); this is because B_i increases with F (see Section 2.4) and F can vary significantly. Assuming the
764 ecosystem is in equilibrium, the respiration of organic carbon on the seafloor can be used to estimate F . Using the
765 large collection of globally distributed Sediment Community Oxygen Consumption (SCOC) data (Stratmann et al.,
766 2019), and limiting to sites less than 6000m in depth and accepting only in situ measurements, SCOC ranges from
767 0.14-110 mmol O₂ m⁻² d⁻¹ (2.5% and 97.5% confidence levels). Excluding shelf regions (<200m depth) reduces the
768 range to 0.08-12 mmol O₂ m⁻² d⁻¹, but it still spans several orders of magnitude. (Note that this result is unaffected by
769 the units as typically a constant factor is used to convert to carbon units.) ~~Such large~~ variations in POC flux would
770 induce similar variability in the longevity of organisms of the same size between different locations if a quadratic
771 mortality parameterisation was used. Therefore, using the linear form of mortality in BORIS-2 avoids a much larger
772 inter-site variability in mortality rate than is currently supported by observations.

773 (3) Observational constraints

774 BORIS-1 was compared to size-resolved data from 3 locations: FG, FSC and OM. While they do contrast in depth
775 and temperature (Table 2) they do not represent the deep seafloor that covers much of the globe. For BORIS-2,
776 additional data from CCZ and PAP are used giving data from two abyssal locations of contrasting food supply. For
777 BORIS-1, the assumption of a fraction respired by non-modelled organisms meant that a comparison to observations
778 of POC flux would be quite subjective. With this restriction removed in BORIS-2 the modelled POC flux is now
779 compared to 2 independent estimates of POC flux at 4 sites and 3 estimates at PAP. For BORIS-1 additional
780 constraints regarding the exponents for size scaling were imposed (see (4) below), as well as a range of expected
781 values for smallest (meiofauna) and largest (macrofauna) organisms. A similar thing to the latter is done for BORIS-
782 2 but, by necessity, for much smaller (bacteria) and larger (megafauna) organisms because of the expanded size range.
783 An additional constraint for BORIS-2 is provided by estimates of TOC in seafloor sediment, which provide a
784 constraint on R .

785 (4) Method of selecting parameter values
786 BORIS-2 has one fewer parameter (7) than BORIS-1 (8). This is despite BORIS-2 incorporating two new processes:
787 temperature sensitive physiology and interference. Without these additions BORIS-2 would have 5 parameters. To
788 find suitable parameter values for ~~Because of the more limited data available to constrain BORIS-1 and the greater~~
789 ~~number of parameters, it was more difficult to find suitable parameter values. To assist in this~~ an optimisation
790 algorithm was ~~therefore~~ used. With fewer parameters and a greater set of constraints this was not necessary for
791 BORIS-2. While it might be possible to construct a similar optimisation routine for BORIS-2, it currently does not
792 warrant the effort, particularly given the ~~subjectivity~~ subjectivity in constructing the necessary cost-function for the
793 optimisation. The user can easily explore parameter space and make a decision on the most suitable parameter values
794 simply using Figure 32 and 43.

795

796 **Code and data availability**

797 All code and data for generating the figures in this paper and for using BORIS either at steady state or dynamically are
798 available on Zenodo at <https://doi.org/10.5281/zenodo.19235638> ~~10.5281/zenodo.15280650~~ (Martin et al., 2026~~5~~). A user
799 manual can be found in the Supplement to this manuscript.

800 **Author contribution**

801 AM was responsible for Writing the original draft and for Software, Validation and Visualisation. AB assisted in model
802 development, testing and sensitivity analysis. All authors were involved in the Conceptualization and Methodology,
803 contributing to the design of the model, and in the review and editing of the Writing. AY, AB, BJB, JD, and SO provided
804 advice related to the Validation of the model.

805 **Competing interests**

806 One author (AY) is a member of the editorial board of journal "Geoscientific Model Development".

807 **Acknowledgements**

808 This work was supported by the NERC National Capability funded CLASS project (NE/R015953/1), the NERC AtlantiS
809 (Atlantic Climate and Environment Impacts) programme ([https://noc.ac.uk/projects/atlantic-climate-environment-strategic-](https://noc.ac.uk/projects/atlantic-climate-environment-strategic-science)
810 [science](https://noc.ac.uk/projects/atlantic-climate-environment-strategic-science), NE/Y005589/1) and the NERC SMARTEX project (NE/T003537/1).

811

812 **References**

- 813 Atwood, T. B., Witt, A., Mayorga, J., Hammill, E. and Sala, E.: Global patterns in marine sediment carbon stocks, *Front. Mar.*
814 *Sci.*, 7, 165, doi: 10.3389/fmars.2020.00165, 2020.
- 815 Benoist, N.: Advances in the state-of-the-art in the quantitative ecology of the marine megabenthos, PhD thesis, University of
816 Southampton, 289 pages, 2020
- 817 Benoist, N. M. A., Bett, B.J., Morris, K.J. and Ruhl, H.A.: A generalised volumetric method to estimate the biomass of
818 photographically surveyed benthic megafauna, *Progress in Oceanography*, 178, 102188, doi: 10.1016/j.pocean.2019.102188,
819 2019
- 820 Best, M. A., Wither, A. W. and Coates, S.: Dissolved oxygen as a physico-chemical supporting element in the Water
821 Framework Directive, *Marine Pollution Bulletin*, 55, 1–6, doi: 10.1016/j.marpolbul.2006.08.037, 2007.

822 Bett, B.J.: UK Atlantic Margin Environmental Survey: Introduction and overview of bathyal benthic ecology, *Continental*
823 *Shelf Research*, 21, 917-956, doi: 10.1016/S0278-4343(00)00119-9, 2001.

824 Blanchard, J. L., et al.: How does abundance scale with body size in coupled size-structured food webs?, *Journal of Animal*
825 *Ecology* 78(1), 270-280, 2009.

826

827 Blanchard, J.L., Law, R., Castle, M.D. et al.: Coupled energy pathways and the resilience of size-structured food webs,
828 *Theoretical Ecology*, 4, 289–300, doi.org/10.1007/s12080-010-0078-9, 2011

829 Brey, T.: An empirical model for estimating aquatic invertebrate respiration, *Methods in Ecology and Evolution*, 1, 92-101,
830 doi:10.1111/j.2041-210X.2009.00008.x, 2010

831 Brey, T.: A multi-parameter artificial neural network model to estimate macrobenthic invertebrate productivity and production.
832 *Limnology and Oceanography: Methods*, 10, 581-589, doi.org/10.4319/lom.2012.10.581, 2012

833 Brown, J.H., Gillooly, J.F., Allen, A.P., Savage, V.M., and West, G.B.: Toward a metabolic theory of ecology. *Ecology*, 85,
834 1771-1789, doi: 10.1890/03-9000, 2004.

835 Burd, A. B.: Modeling the vertical flux of organic carbon in the global ocean, *Annual Review of Marine Science*, 16, 135-161.
836 doi.org/10.1146/annurev-marine-022123-102516, 2024

837 Busecke, J. J. M., Resplandy, L., Ditkovsky, S. J., and John, J. G.: Diverging fates of the Pacific Ocean Oxygen Minimum
838 Zone and its core in a warming world, *AGU Advances*, 3(6), e2021AV000470. doi: 10.1029/2021AV000470, 2022.

839 Butenschön, M., Clark, J., Aldridge, J.N., Allen, J.I., Artioli, Y., Blackford, J., Bruggeman, J., Cazenave, P., Ciavatta, S., Kay,
840 S., Lessin, G., van Leeuwen, S., van der Molen, J., de Mora, L., Polimene, L., Saille, S., Stephens, N., Torres, R.: ERSEM
841 15.06: a generic model for marine biogeochemistry and the ecosystem dynamics of the lower trophic levels, *Geoscientific*
842 *Model Development*, 9(4), 1293–1339, doi: 10.5194/gmd-9-1293-2016, 2016

843 Childress, J. J. and B. A. Seibel: Life at stable low oxygen levels: adaptations of animals to oceanic oxygen minimum layers,
844 *Journal of Experimental Biology* 201(8), 1223-1232, 1998.

845 Cooley, S., D. Schoeman, L. Bopp, P. Boyd, S. Donner, D.Y. Ghebrehiwet, S.-I. Ito, W. Kiessling, P. Martinetto, E. Ojea, M.-
846 F. Racault, B. Rost, and M. Skern-Mauritzen: Ocean and Coastal Ecosystems and their Services. In: *Climate Change 2022:*
847 *Impacts, Adaptation, and Vulnerability. Contribution of Working Group II to the Sixth Assessment Report of the*
848 *Intergovernmental Panel on Climate Change* [H.-O. Pörtner, D.C. Roberts, M. Tignor, E.S. Poloczanska, K. Mintenbeck, A.
849 Alegria, M. Craig, S. Langsdorf, S. Löschke, V. Möller, A. Okem, B. Rama (eds.)]. Cambridge University Press, Cambridge,
850 UK and New York, NY, USA, pp. 379-550, doi:10.1017/9781009325844.005, 2022.

851 Cusson, M., & Bourget, E.: Global patterns of macroinvertebrate production in marine benthic habitats [Review]. *Marine*
852 *Ecology Progress Series*, 297, 1-14. doi.org/10.3354/meps297001, 2005.

853 Damuth J.: A macroevolutionary explanation for energy equivalence in the scaling of body size and population density, *Am.*
854 *Nat.*, 169, 621-31, doi: 10.1086/513495, 2007.

855 DeAngelis, D. L., Goldstein, R. A., and O'Neill, R. V.: A Model for trophic interaction, *Ecology*, 56(4), 881–892.
856 doi.org/10.2307/1936298, 1975.

857 de Jonge, D. S. W., Stratmann, T., Lins, L., Vanreusel, A., Purser, A., Marcon, Y., Rodrigues, C. F., Ravara, A., Esquete, P.,
858 Cunha, M. R., Simon-Lledó, E., van Breugel, P., Sweetman, A. K., Soetaert, K. and van Oevelen, D.: Abyssal food-web model
859 indicates faunal carbon flow recovery and impaired microbial loop 26 years after a sediment disturbance experiment, *Progress*
860 *in Oceanography*, 189, 102446, doi.org/10.1016/j.pocean.2020.102446, 2020.

861 Demopoulos, A. W. J., Smith, C. R., and Tyler, P. A.: The deep Indian Ocean floor, p. 219–237. In P. A. Tyler [ed.],
862 *Ecosystems of the world 28. Ecosystems of the deep oceans*. Elsevier, 2003.

863 Dixon, J. L. and Turley, C. M.: Measuring bacterial production in deep-sea sediments using ³H-Thymidine incorporation:
864 ecological significance, *Microbial Ecology*, 42(4), 549-561, 2001

865 Dunne, J. P., Sarmiento, J. L. and Gnanadesikan, A.: A synthesis of global particle export from the surface ocean and cycling
866 through the ocean interior and on the seafloor, *Global Biogeochemical Cycles*, 21(4), doi.org/10.1029/2006GB002907, 2007.

867 Durden, J.M., Bett, B.J., Ruhl, H.A.: The hemisessile lifestyle and feeding strategies of *Iosactis vagabunda* (Actiniaria,
868 Iosactiidae), a dominant megafaunal species of the Porcupine Abyssal Plain, *Deep-Sea Research Part I*, 102, 72-77.
869 10.1016/j.dsr.2015.04.010, 2015.

870 Durden, J.M., Ruhl, H.A., Pebody, C., Blackbird, S.J. and van Oevelen, D.: Differences in the carbon flows in the benthic food
871 webs of abyssal hill and plain habitats, *Limnology and Oceanography*, 62 (4). 1771-1782. doi.org/10.1002/lno.10532, 2017.

872 Durden, J.M., Bett, B.J., Huffard, C., Ruhl, H.A., and Smith Jr, K.L.: Abyssal deposit-feeding rates consistent with the
873 Metabolic Theory of Ecology, *Ecology*, 100, e02564. 10.1002/ecy.2564, 2019.

874 Durden, J.M., Bett, B.J., Huffard, C.L., Pebody, C., Ruhl, H.A., and Smith, K.L.: Response of deep-sea deposit-feeders to
875 detrital inputs: A comparison of two abyssal time-series sites. *Deep Sea Research Part II*, 173, 104677.
876 10.1016/j.dsr2.2019.104677, 2020a.

877 Durden, J. M., Bett, B. J. and Ruhl, H.A.: Subtle variation in abyssal terrain induces significant change in benthic megafaunal
878 abundance, diversity, and community structure, *Prog. Oceanogr.*, 186, 102395, doi: 10.1016/j.pocean.2020.102395, 2020b.

879 Edwards, A.M., Robinson, J.P.W., Plank, M.J., Baum, J.K. and Blanchard, J.L.: Testing and recommending methods for fitting
880 size spectra to data, *Methods Ecol. Evol.*, 8, 57-67, doi: 10.1111/2041-210X.12641, 2017.

881 Edwards, A.M., Robinson, J.P.W., Blanchard, J.L., Baum, J.K. and Plank M.J.: Accounting for the bin structure of data
882 removes bias when fitting size spectra, *Mar. Ecol. Prog. Ser.*, 636,19-33, doi: 10.3354/meps13230, 2020.

883 Ehrnsten, E., Norkko, A., Timmermann, K. and Gustafsson, B. G.: Benthic-pelagic coupling in coastal seas – Modelling
884 macrofaunal biomass and carbon processing in response to organic matter supply, *Journal of Marine Systems*, 196, 36-47,
885 2018.

886 Ernest, S. K. M., Enquist, B. J., Brown, J. H., Charnov, E. L., Gillooly, J. F., Savage, V. M., White, E. P., Smith, F. A., Hadly,
887 E. A., Haskell, J. P., Lyons, S. K., Maurer, B. A., Niklas, K. J. and Tiffney, B.: Thermodynamic and metabolic effects on the
888 scaling of production and population energy use, *Ecology Letters*, 6(11), 990-995, doi.org/10.1046/j.1461-0248.2003.00526.x,
889 2003

890 Garry, F. K., McDonagh, E. L., Blaker, A. T., Roberts, C. D., Desbruyères, D. G., Frajka-Williams, E., King, B. A.: Model-
891 derived uncertainties in deep ocean temperature trends between 1990 and 2010, *Journal of Geophysical Research: Oceans*,
892 124, 1155–1169. doi: 10.1029/2018JC014225, 2019.

893 Gillooly J.F., Brown, J.H., West, G.B., Savage, V.M. and Charno, E.L.: Effects of Size and Temperature on Metabolic Rate,
894 *Science*, 293, 2248-2251, doi: 10.1126/science.1061967, 2001

895 [Giovannelli, D., Molari, M., d’Errico, G., Baldrighi, E., Pala, C., Manini, E.: Large-Scale Distribution and Activity of](#)
896 [Prokaryotes in Deep-Sea Surface Sediments of the Mediterranean Sea and the Adjacent Atlantic Ocean, PLoS ONE, 8,](#)
897 [10.1371/journal.pone.0072996, 2013](#)

898 Glazier, D. S.: Variable metabolic scaling breaks the law: from ‘Newtonian’ to ‘Darwinian’ approaches, *Proc. R. Soc.*
899 *B*.28920221605, doi.org/10.1098/rspb.2022.1605, 2022.

900 Harris, P.T., Macmillan-Lawler, M., Rupp, J., and Baker, E.K. Geomorphology of the oceans. *Marine Geology*, 352, 4-24.
901 10.1016/j.margeo.2014.01.011, 2014.

902 Hartman, S.E., Bett, B.J., Durden, J.M., Henson, S.A., Iversen, M., Jeffrey, R.M., Horton, T., Lampitt, R., and Gates, A.R.:
903 Enduring science: Three decades of observing the Northeast Atlantic from the Porcupine Abyssal Plain Sustained Observatory
904 (PAP-SO), *Progress in Oceanography*, 191, 102508, doi: 10.1016/j.pocean.2020.102508, 2021.

905 [Hatton, I. A., Heneghan, R. F., Bar-On, Y. M., & Galbraith, E. D.: The global ocean size spectrum from bacteria to whales.](#)
906 [Science Advances, 7, 10.1126/sciadv.abh3732, 2021](#)

907 Henson, S.A., Laufkötter, C., Leung, S. et al.: Uncertain response of ocean biological carbon export in a changing world. *Nat.*
908 *Geosci.* 15, 248–254, doi.org/10.1038/s41561-022-00927-0, 2022

909 Iken, K., Brey, T., Wand, U., Voigt, J., and Junghans, P.: Food web structure of the benthic community at the Porcupine
910 Abyssal Plain (NE Atlantic): a stable isotope analysis, *Progress in Oceanography*, 50, 383-405, doi: 10.1016/S0079-
911 6611(01)00062-3, 2001.

912 Isaac, N.J.B., Carbone, C.: Why are metabolic scaling exponents so controversial? Quantifying variance and testing
913 hypotheses. *Ecology Letters*, 13, 728-735. 10.1111/j.1461-0248.2010.01461.x, 2010.

914 Jones, D.O.B., Yool, A., Wei, C.-L., Henson, S.A., Ruhl, H.A., Watson, R.A. and Gehlen, M.: Global reductions in seafloor
915 biomass in response to climate change, *Glob Change Biol*, 20: 1861-1872, doi.org/10.1111/gcb.12480, 2014.

916 Jørgensen, B. B., and Marshall, I. P. G.: Slow Microbial Life in the Seabed. *Annual Review of Marine Science*, 8, 311-332.
917 doi.org/10.1146/annurev-marine-010814-015535, 2016.

918 Kaariainen J. I. and Bett, B. J.: Evidence for benthic body size miniaturization in the deep sea, *Journal of the Marine Biological*
919 *Association of the United Kingdom*, 86, 1339-1345, doi: 10.1017/S0025315406014366, 2006.

920 Karp, M. A. et al.: Increasing the uptake of multispecies models in fisheries management, *ICES Journal of Marine Science*,
921 80(2), 243-257, doi.org/10.1093/icesjms/fsad001, 2023.

922 Kelly-Gerreyn, B. A., Martin, A. P., Bett, B. J., Anderson, T. R., Kaariainen, J. I., Main, C. E., Marcinko, C. J. and Yool, A.:
923 Benthic biomass size spectra in shelf and deep-sea sediments, *Biogeosciences*, 11, 6401-6416, doi:10.5194/bg-11-6401-2014,
924 2014.

925 Kwiatkowski, L., Torres, O., Bopp, L., Aumont, O., Chamberlain, M., Christian, J. R., Dunne, J. P., Gehlen, M., Ilyina, T.,
926 John, J. G., Lenton, A., Li, H., Lovenduski, N. S., Orr, J. C., Palmieri, J., Santana-Falcón, Y., Schwinger, J., Séférian, R.,
927 Stock, C. A., Tagliabue, A., Takano, Y., Tjiputra, J., Toyama, K., Tsujino, H., Watanabe, M., Yamamoto, A., Yool, A., and
928 Ziehn, T.: Twenty-first century ocean warming, acidification, deoxygenation, and upper-ocean nutrient and primary production
929 decline from CMIP6 model projections, *Biogeosciences*, 17, 3439–3470, <https://doi.org/10.5194/bg-17-3439-2020>, 2020.

930 Laguionie Marchais, C., Bett, B. J., Paterson, G. L. J., Smith, K. L., and Ruhl, H. A.: Using metabolic theory to assess structure
931 and function in the deep-sea benthos, including microbial and metazoan dominance, *Deep-Sea Research II*, 173, 104762. doi:
932 10.1016/j.dsr2.2020.104762, 2020.

933 [Lampitt, R.S., Newton, P.P., Jickells, T.D., Thomson, J., King, P.: Near-bottom particle flux in the abyssal northeast Atlantic.](#)
934 [Deep Sea Research Part II, 47, Issues 9–11, 10.1016/S0967-0645\(00\)00016-3, 2000](#)

935 [Lampitt, R.S., Bett, B.J., Kiriakoulakis, K., Popova, E.E., Ragueneau, O., Vangriesheim, A., and Wolff, G.A.: Material supply](#)
936 [to the abyssal seafloor in the Northeast Atlantic, Progress in Oceanography, 50, 10.1016/S0079-6611\(01\)00047-7, 2001.](#)

937 Lampitt R.S., and Pebody C.A.: Sediment Trap data from the Porcupine Abyssal Plain Sustained Observatory (PAP-SO) site
938 on PAP3 mooring at 3000 metres April 1989 - June 2019 Version 2. NERC EDS British Oceanographic Data Centre NOC.
939 doi:10.5285/06bd25d5-fcd3-0f63-e063-6c86abc0481e, 2023.

940 Lampitt, R.S., Briggs, N., Cael, B.B., Espinola, B., Hélaouët, P., Henson, S.A., Norrbin, F., Pebody, C.A. and Smeed, D.:
941 Deep ocean particle flux in the Northeast Atlantic over the past 30 years: carbon sequestration is controlled by ecosystem
942 structure in the upper ocean, *Front. Earth Sci.*, 11:1176196, doi: 10.3389/feart.2023.1176196, 2023.

943 Levin, L.A.: Oxygen minimum zone Benthos: Adaptation and community response to hypoxia, *Oceanography and Marine*
944 *Biology*, 41, 1-45, 2003.

945 Luef, B., Frischkorn, K. R., Wrighton, K. C., Holman, H.-Y. N., Birarda, G., Thomas, B. C., Singh, A., Williams, K. H.,
946 Siegerist, C. E., Tringe, S. G., Downing, K. H., Comolli, L. R. and Banfield, J. F.: Diverse uncultivated ultra-small bacterial
947 cells in groundwater, *Nature Communications*, 6(1), 6372, doi.org/10.1038/ncomms7372, 2015

948 Lutz, M. J., Caldeira, K., Dunbar, R.B., and Behrenfeld, M.J.: Seasonal rhythms of net primary production and

949 particulate organic carbon flux to depth describe the efficiency of biological pump in the global ocean, *J. Geophys. Res.*, 112,
950 C10011, doi:10.1029/2006JC003706, 2007

951 McCarthy J. K., Dwyer J. M. and Mokany, K.: A regional-scale assessment of using metabolic scaling theory to predict
952 ecosystem properties, *Proc. R. Soc. B.*28620192221, doi.org/10.1098/rspb.2019.2221, 2019.

953 McClain, C.R., Allen, A.P., Tittensor, D.P., and Rex, M.A.: Energetics of life on the deep seafloor, *Proceedings of the National
954 Academy of Sciences*, 109, 15366-15371. 10.1073/pnas.1208976109, 2012.

955 McCoy, M. W. and Gillooly, J. F.: Predicting natural mortality rates of plants and animals, *Ecology Letters*, 11(7), 710-716,
956 doi.org/10.1111/j.1461-0248.2008.01190.x, 2008.

957 McCoy, M. W. and Gillooly, J. F.: Predicting natural mortality rates of plants and animals, *Corrigendum, Ecology Letters*,
958 12(7), 731-733, doi.org/10.1111/j.1461-0248.2009.01338.x, 2009

959 Mahaut, M. L., Sibuet, M. and Shirayama, Y.: Weight-dependent respiration rates in deep-sea organisms, *Deep Sea Research
960 Part I*, 42(9), 1575-1582, 1995.

961 Martin, A. P., Benoist, N., Bett, B. J., Brombacher, A., Durden, J., Oliver, S., and Yool, A.: Matlab code associated with the
962 BORIS-2 benthic ecosystem model, Zenodo,
963 ~~<https://doi.org/10.5281/zenodo.15280650>~~<https://doi.org/10.5281/zenodo.19235638>, 20265.

964 Martin, J. H., Knauer, G. A., Karl, D. M., and Broenkow, W. W.: VERTEX: carbon cycling in the northeast Pacific, *Deep Sea
965 Research Part A.*, 34(2), 267-285, doi.org/10.1016/0198-0149(87)90086-0, 1987.

966 Molony, C.L., Field, J.G.: General allometric equations for rates of nutrient uptake, ingestion, and respiration in plankton
967 organisms. *Limnology Oceanography*, 34, 1290-1299, 1989.

968 Moore, C. G. and Bett, B. J.: The use of meiofauna in marine pollution impact assessment, *Zoological Journal of the Linnean
969 Society*, 96, 263–280, doi: 10.1111/j.1096-3642.1989.tb02260.x, 1989.

970 Morris, K. J., Bett, B. J., Durden, J. M., Benoist, N. M. A., Huvenne, V. A. I., Jones, D. O. B., Robert, K., Ichino, M. C., Wolff,
971 G. A., Ruhl, H. A.: Landscape-scale spatial heterogeneity in phytodetrital cover and megafauna biomass in the abyss links to
972 modest topographic variation. *Sci Rep* 6, 34080. Doi: 10.1038/srep34080, 2016.

973 Nagy, K.A.: Field Metabolic Rate and Food Requirement Scaling in Mammals and Birds. *Ecological Monographs*, 57, 112-
974 128. 10.2307/1942620, 1987.

975 Niven, J. E. and Scharlemann, J. P.W.: Do insect metabolic rates at rest and during flight scale with body mass? *Biol.
976 Lett.*1346–349, doi.org/10.1098/rsbl.2005.0311, 2005.

977 Nowicki, M., DeVries, T. and Siegel, D. A.: Quantifying the Carbon Export and Sequestration Pathways of the Ocean's
978 Biological Carbon Pump, *Global Biogeochemical Cycles*, 36(3), e2021GB007083, doi.org/10.1029/2021GB007083, 2022

979 Parameswaran, N., González, E., Burwicz-Galerie, E., Braack, M., and Wallmann, K.: NN-TOC v1: global prediction of total
980 organic carbon in marine sediments using deep neural networks, *EGU sphere [preprint]*, [https://doi.org/10.5194/egusphere-
981 2024-1360](https://doi.org/10.5194/egusphere-2024-1360), 2024.

982 Pearson, T.H. and Rosenberg, R.: Macrobenthic Succession in Relation to Organic Enrichment and Pollution of the Marine
983 Environment. *Oceanography and Marine Biology—An Annual Review*, 16, 229-311, 1978.

984 O’Dor, R.K., Fennel, K. and Berghe, E. V.: A one ocean model of biodiversity, *Deep Sea Research Part II*, 56, 1816-1823,
985 doi.org/10.1016/j.dsr2.2009.05.023, 2009.

986 Quiroga, E., Quiñones, R., Palma, M., Sellanes, J., Gallardo, V.A., Gerdes, D., Rowe, G.: Biomass size-spectra of
987 macrobenthic communities in the oxygen minimum zone off Chile, *Estuarine, Coastal and Shelf Science*, 62(1), 217-231, 2005

988 Reagan, J. R., Boyer, T. P., García, H. E., Locarnini, R. A., Baranova, O. K., Bouchard, C., Cross, S. L., Mishonov, A. V.,
989 Paver, C. R., Seidov, D., Wang, Z., Dukhovskoy, D.: *World Ocean Atlas 2023*. NOAA National Centers for Environmental
990 Information. Dataset: NCEI Accession 0270533, 2024

991 Ramirez-Llodra, E., Brandt, A., Danovaro, R., De Mol, B., Escobar, E., German, C.R., Levin, L.A., Arbizu, P.M., Menot, L.,
992 Buhl-Mortensen, P., Narayanaswamy, B.E., Smith, C.R., Tittensor, D.P., Tyler, P.A., Vanreusel, A., Vecchione, M.: Deep,
993 diverse and definitely different: unique attributes of the world's largest ecosystem. *Biogeosciences*, 7, 2851-2899, 2010.
994 10.5194/bg-7-2851-2010

995 Reiss, H., et al.: Benthos distribution modelling and its relevance for marine ecosystem management, *Ices Journal of Marine*
996 *Science*, 72(2), 297-315, 2014.

997 Ruhl, H. A.: Community change in the variable resource habitat of the abyssal northeast Pacific, *Ecology*, 89(4), 991-1000,
998 2008.

999 Ruhl, H. A., Ellena, J. A., and Smith, Jr, K. J.: Connections between climate, food limitation, and carbon cycling in abyssal
1000 sediment communities, *Proceedings of the National Academy of Sciences*, 105(44), 17006-17011, 2008.

1001 Ruhl, H.A., Bett, B.J., Ingels, J., Martin, A., Gates, A.R., Yool, A., Benoist, N.M.A., Appeltans, W., Howell, K.L., Danovaro,
1002 R.: Integrating ocean observations across body-size classes to deliver benthic invertebrate abundance and distribution
1003 information. *Limnol. Oceanogr. Lett.*, 8, 692-706, doi: 10.1002/lol2.10332, 2023.

1004 Savage, Van M., Gillooly, James F., Brown, James H., West, Geoffrey B. and Charnov, Eric L.: Effects of Body Size and
1005 Temperature on Population Growth. *The American Naturalist*, 163(3), 429-441, doi.org/10.1086/381872, 2004

1006 Seibel, B.A., and Drazen, J.C.: The rate of metabolism in marine animals: environmental constraints, ecological demands and
1007 energetic opportunities. *Philosophical Transactions of the Royal Society B: Biological Sciences*, 362, 2061-2078.
1008 10.1098/rstb.2007.2101, 2007.

1009 Simon-Lledó, E., Bett, B. J., Huvenne, V. A. I., Schoening, T., Benoist, N. M. A., Jeffrey, R. M., Durden, J. M., Jones, D. O.
1010 B.: Megafaunal variation in the abyssal landscape of the Clarion Clipperton Zone, *Progress in Oceanography*, 170, 119-133,
1011 doi: 10.1016/j.pocean.2018.11.003, 2019

1012 Smith, C. R., De Leo, F. C., Bernardino, A. F., Sweetman, A. K. and Arbizu, P. M.: Abyssal food limitation, ecosystem
1013 structure and climate change, *Trends in Ecology & Evolution*, 23(9), 518-528, doi.org/10.1016/j.tree.2008.05.002, 2008

1014 Smith, K.L., Ruhl, H.A., Kahru, M., Huffard, C.L., Sherman, A.D.: Deep ocean communities impacted by changing climate
1015 over 24 y in the abyssal northeast Pacific Ocean, *Proceedings of the National Academy of Sciences*, 110.
1016 10.1073/pnas.1315447110, 2013.

1017 Soetaert, K., and van Oevelen, D.: Modeling food web interactions in benthic deep-sea ecosystems: A practical guide,
1018 *Oceanography*, 22(1), 128–143, <https://doi.org/10.5670/oceanog.2009.13>, 2009.

1019 Stratmann, T., et al.: The SCOC database, a large, open, and global database with sediment community oxygen consumption
1020 rates, *Scientific Data* 6(1), 242, 2019.

1021 [Sweetman, A.K., Smith, C.R., Shulse, C.N., Maillot, B., Lindh, M., Church, M.J., Meyer, K.S., van Oevelen, D., Stratmann,](#)
1022 [T. and Gooday, A.J.: Key role of bacteria in the short-term cycling of carbon at the abyssal seafloor in a low particulate organic](#)
1023 [carbon flux region of the eastern Pacific Ocean. *Limnol Oceanogr*, 64, 10.1002/lno.11069, 2019.](#)

1024 Turrell, W. R., Slessor, G., Adams, R. D., Payne, R., and Gillibrand, P. A.: Decadal variability in the composition of Faroe
1025 Shetland Channel bottom water. *Deep Sea Research I*, 46, 1-25. doi: 10.1016/S0967-0637(98)00067-3, 1999.

1026 van Oevelen, D., Soetaert, K., Garcia, R., de Stigter, H. C., Cunha, M. R., Pusceddu, A. and Danovaro, R.: Canyon conditions
1027 impact carbon flows in food webs of three sections of the Nazaré canyon, *Deep Sea Research Part II: Topical Studies in*
1028 *Oceanography*, 58(23), 2461-2476, doi.org/10.1016/j.dsr2.2011.04.009, 2011a

1029 van Oevelen, D., Bergmann, M., Soetaert, K., Bauerfeind, E., Hasemann, C., Klages, M., Schewe, I., Soltwedel, T. and
1030 Budaeva, N. E.: Carbon flows in the benthic food web at the deep-sea observatory HAUSGARTEN (Fram Strait). *Deep Sea*
1031 *Research Part I: Oceanographic Research Papers*, 58(11), 1069-1083, doi.org/10.1016/j.dsr.2011.08.002, 2011b.

1032 Vaquer-Sunyer, R. and Carlos M. Duarte: Thresholds of hypoxia for marine biodiversity, *PNAS*, 105, 15452-15457. doi:
1033 10.1073/pnas.0803833105, 2008.

1034 Wei C-L, Rowe G.T., Escobar-Briones E., Boetius A., Soltwedel T., et al.: Global patterns and predictions of seafloor biomass
1035 using random forests, PLoS ONE 5(12), e15323, doi:10.1371/journal.pone.0015323, 2010.

1036 West, G. B., Brown, J. H. and Enquist, B. J.: A General Model for the Origin of Allometric Scaling Laws in Biology, Science,
1037 276(5309), 122-126, 1997.

1038 White, E.P., Ernest, S.K.M., Kerkhoff, A.J., Enquist, B.J.: Relationships between body size and abundance in ecology, Trends
1039 in Ecology & Evolution, 22, 323-330. 10.1016/j.tree.2007.03.007, 2007

1040 [Witte, U., Wenzhöfer, F., Sommer, S., Boetius, A., Heinz, P., Aberle, N., Sand, M., Cremer, A., Abraham, W. R., Jørgensen,](#)
1041 [B. B., and Pfannkuche, O.: In situ experimental evidence of the fate of a phytodetritus pulse at the abyssal sea floor, Nature,](#)
1042 [424, 10.1038/nature01799, 2003.](#)

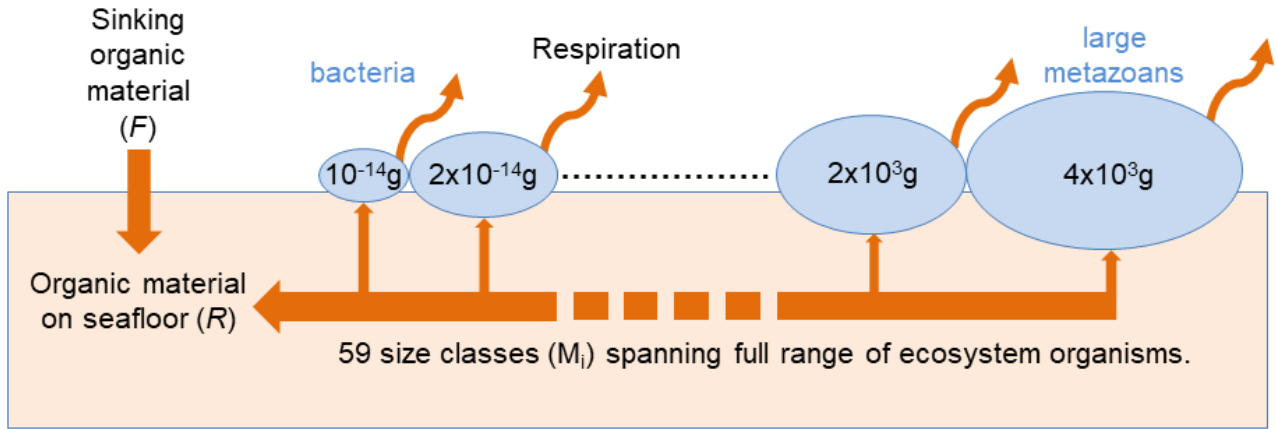
1043 Woodson, C., Schramski, J.R. & Joye, S.B.: A unifying theory for top-heavy ecosystem structure in the ocean. *Nat Commun*
1044 **9**, 23 (2018). <https://doi.org/10.1038/s41467-017-02450-y>, 2018.

1045 Yool, A, Martin, A.P., Anderson, T.R., Bett, B.J., Jones, D.O.B., Ruhl, H.A.: Big in the benthos: Future change of seafloor
1046 community biomass in a global, body size-resolved model, *Global Change Biology*, 23, 3554–3566.
1047 doi.org/10.1111/gcb.13680, 2017

1048

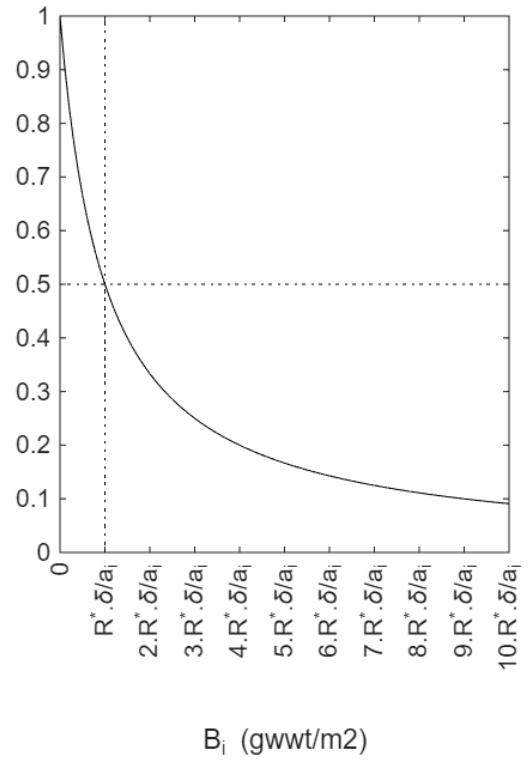
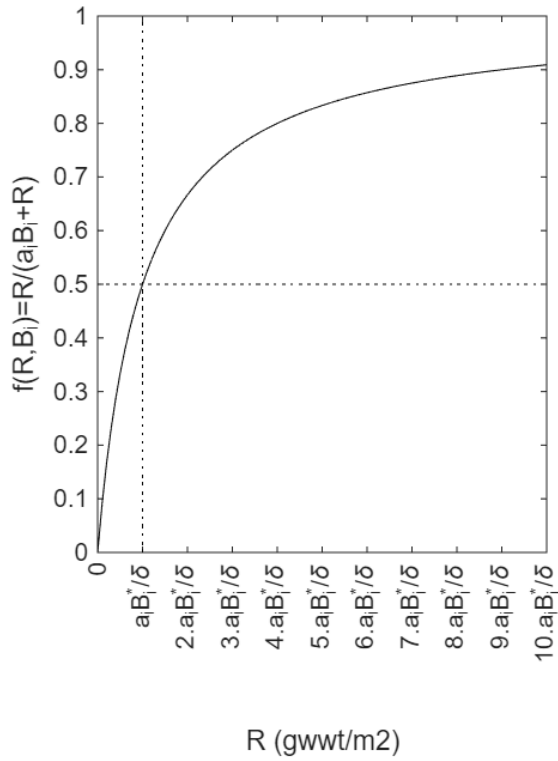
1049

1050



1051

1052 Figure 1: Schematic of BORIS-2. Within each size class (M_i) the total biomass (B_i) is controlled by growth, using organic
1053 material, on the seafloor, and losses to respiration and mortality. Organic material (R) accumulates on the seafloor from the
1054 deposition of sinking particulate organic carbon (F) and mortality of benthic organisms. Growth, respiration and mortality
1055 are all assumed to scale as a ~~power-law~~power-law with M_i and as an exponential function of ambient temperature (see
1056 Section 2). Numbers denote median mass (units: g wet weight) for each size class and example organisms of smallest and
1057 largest size classes are given in blue.
1058



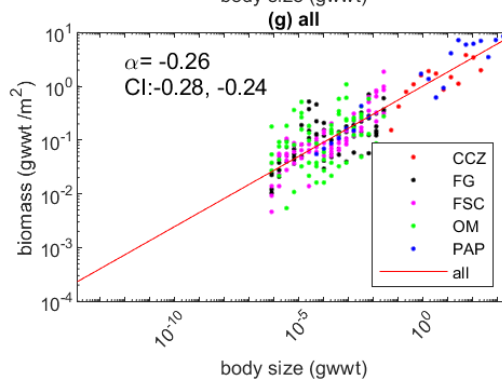
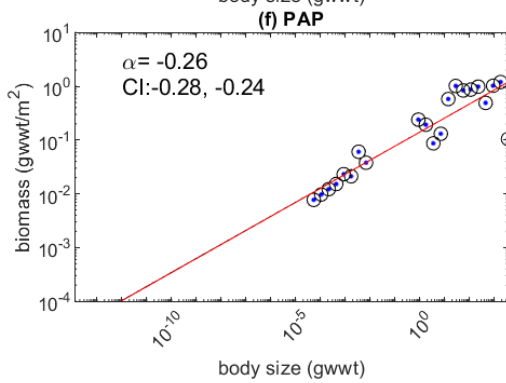
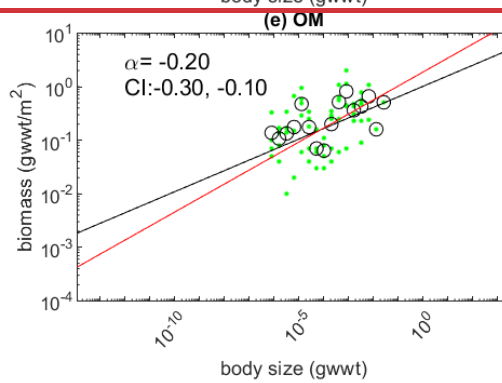
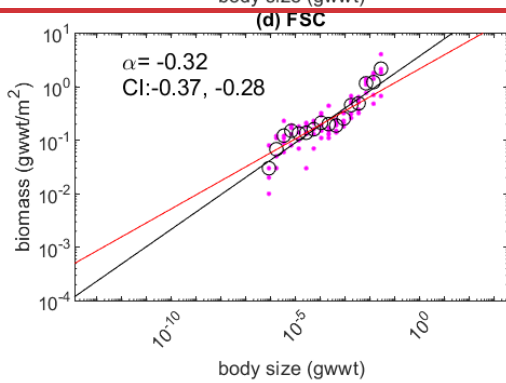
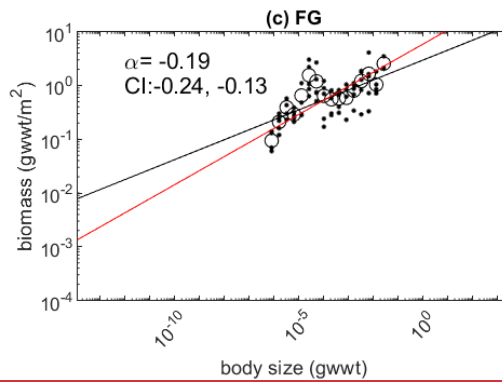
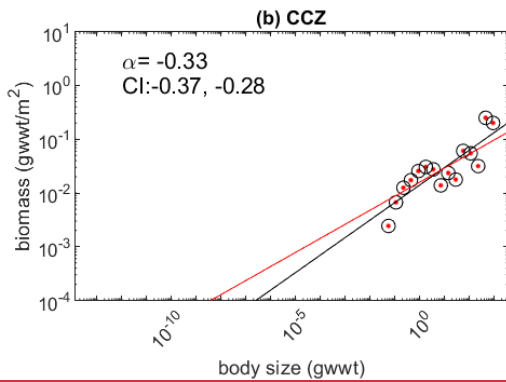
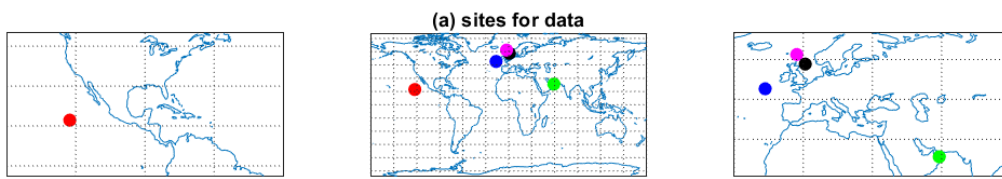
R (gwwt/m2)

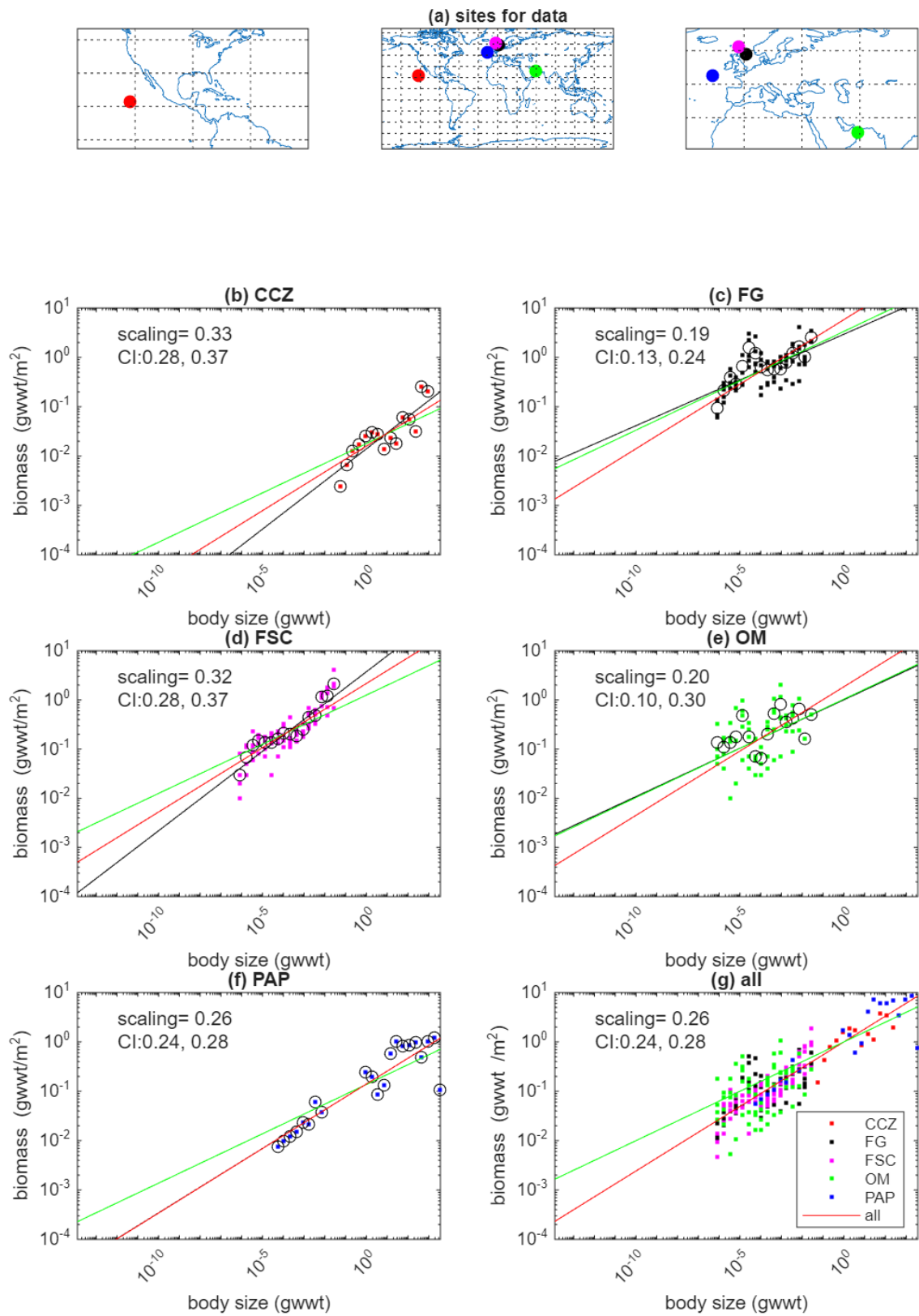
B_i (gwwt/m2)

1059
1060
1061
1062
1063

Figure 2: Plots showing how the growth limitation function, $f(R, B_i) = 1 / (1 + a_i B_i / R)$ varies as either R (left) or B_i (right) is varied. R_i^* and B_i^* denote values at steady state (vertical dotted line), where additionally $\delta R_i^* = a_i B_i^*$. Note that because of the scaling behaviour of a_i , $a_i B_i$ is the same for all i at any site.

1064
1065

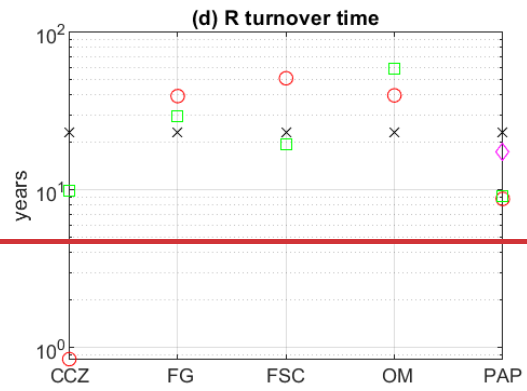
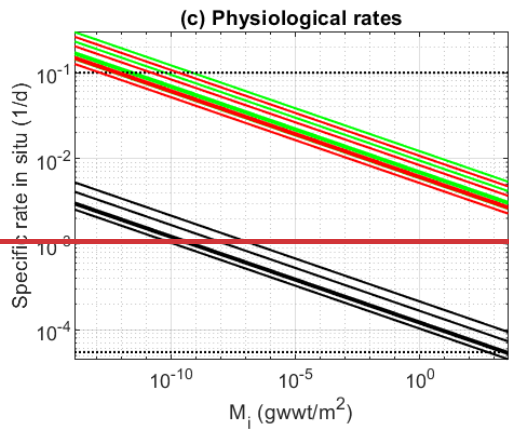
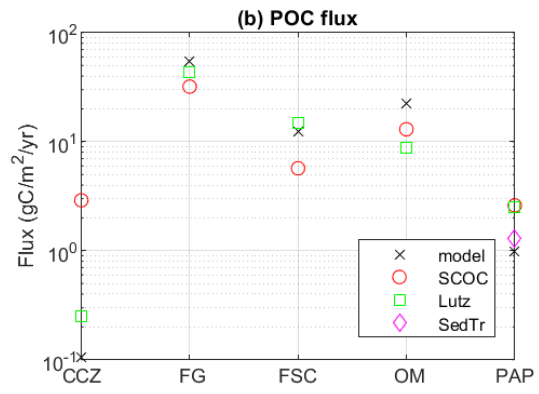
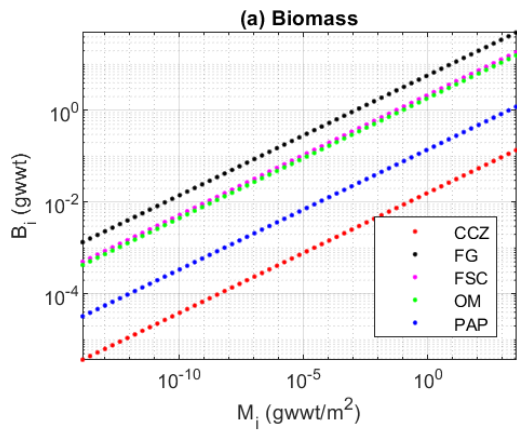




1067

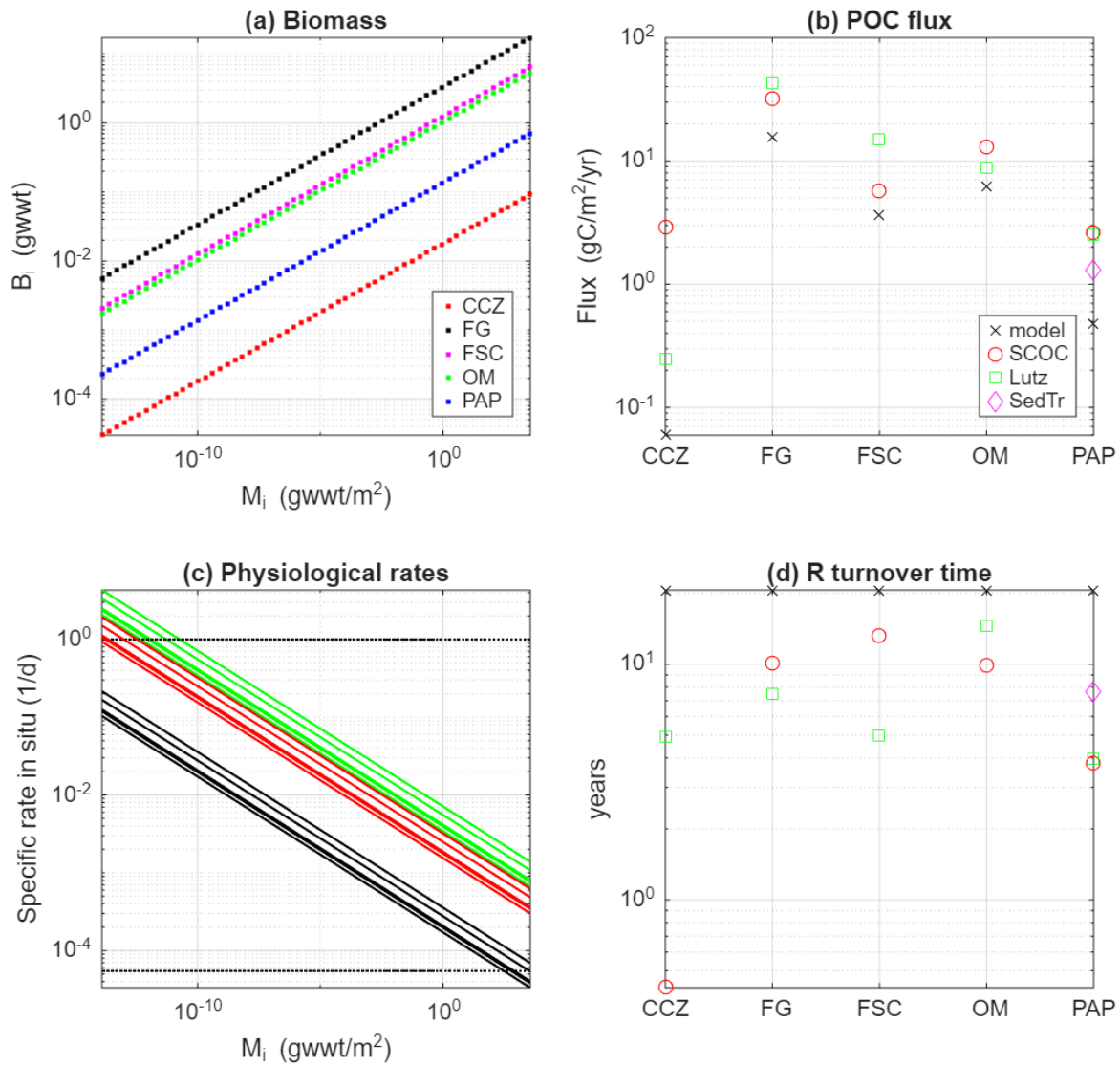
1068

1069 **Figure 32** Locations (top) and observations of biomass as a function of body size for the **five** sites listed in Table 2. For each of the
 1070 **5**-sites the dots show observations, circles indicate means within size classes and the black line is **the a power-law fit of $B=k_j M^{-\alpha}$ to**
 1071 **the observations for the j^{th} site where B is biomass and M is size.** The fitted values for **the scaling exponent** together with 95%
 1072 confidence intervals are also shown. The bottom right panel shows the fit to all sites simultaneously, assuming a common **scaling**
 1073 **exponent** (fitted value shown with 95% CI) but allowing **the pre-factor** to vary across sites. The dots show data from the **5** sites
 1074 with colours matching those used in the panels for individual sites. Note that in the bottom right panel the data from each site has
 1075 been normalised by dividing by the fitted **pre-factor** to allow the visual comparison. The red line in all panels is the simultaneous
 1076 fit to all sites. **The green line in all plots is the relationship used in the model by fitting a power-law with an imposed scaling of 0.2 to**
 1077 **the same observations.**



(e) Table of diagnostics

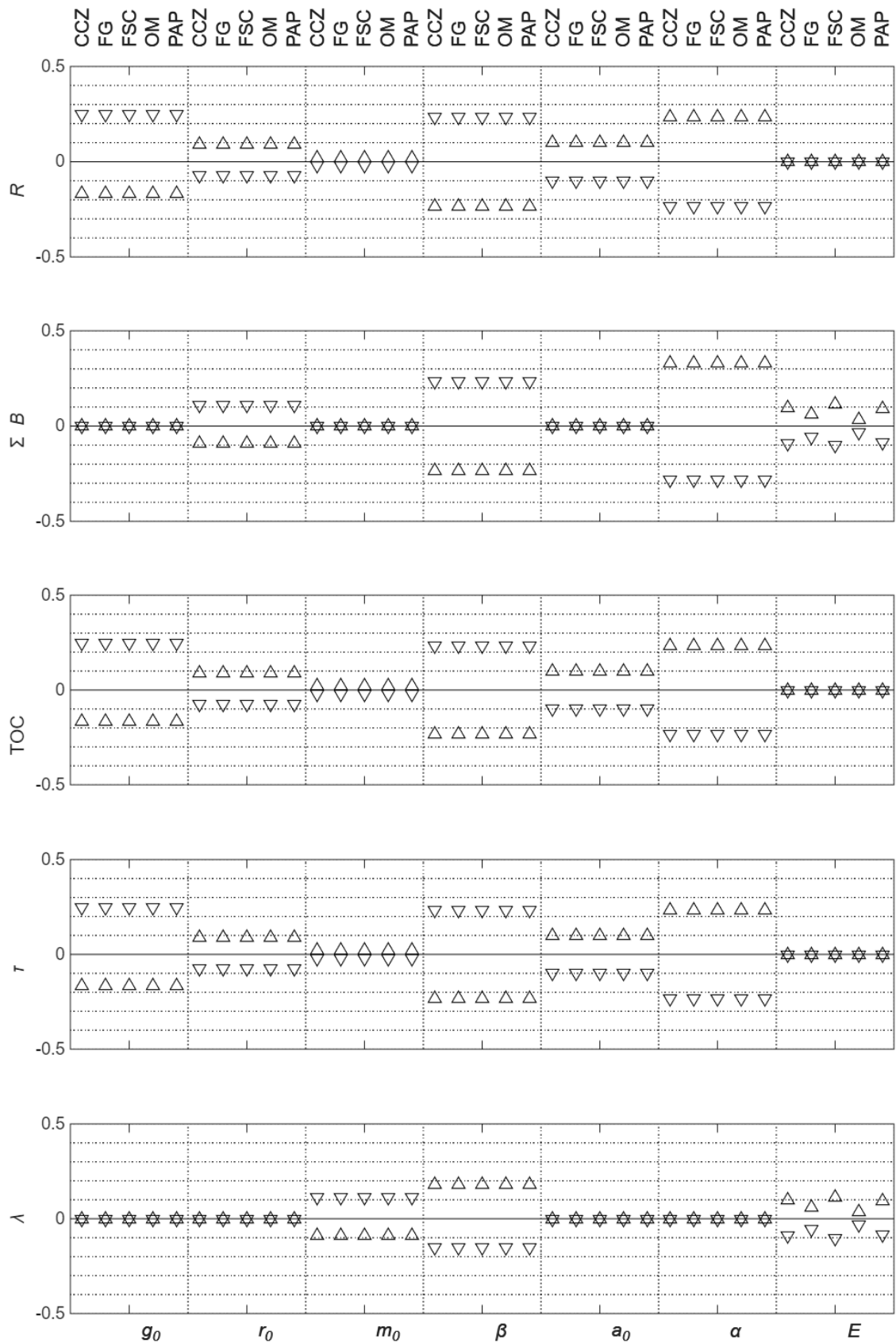
Site	Total	R	TOC	Biggest organism	
	biomass		Model	Obs	lifetime
	gC/m2	gC/m2	gC/m2	gC/m2	yr
CCZ	0.071	2.5	50	400	53
FG	26	1300	26000	800	37
FSC	9.7	290	5800	550	60
OM	8.3	520	10400	2000	29
PAP	0.63	23	460	320	50



(e) Table of diagnostics

Site	Total biomass	R	TOC Model	TOC Obs	Biggest organism lifetime
	gC/m2	gC/m2	gC/m2	gC/m2	yr
CCZ	0.062	1.2	24	400	72
FG	12	320	6400	800	51
FSC	4.3	75	1500	550	82
OM	3.6	130	2600	2000	40
PAP	0.48	9.9	198	320	68

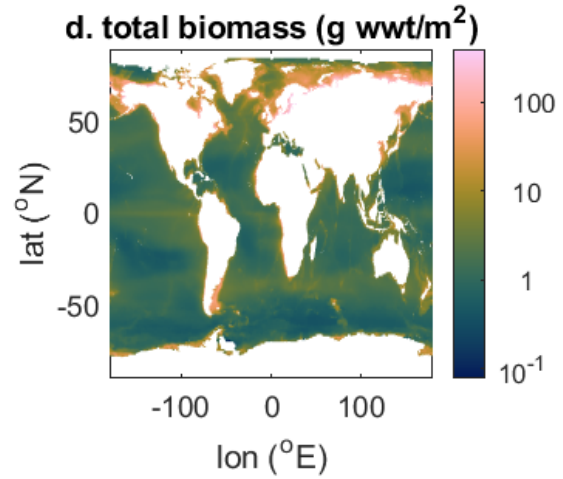
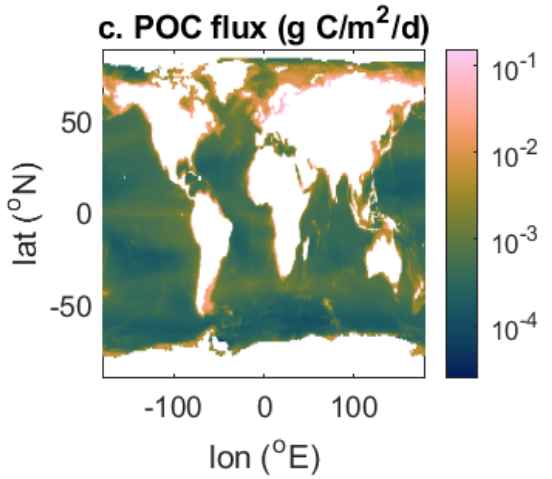
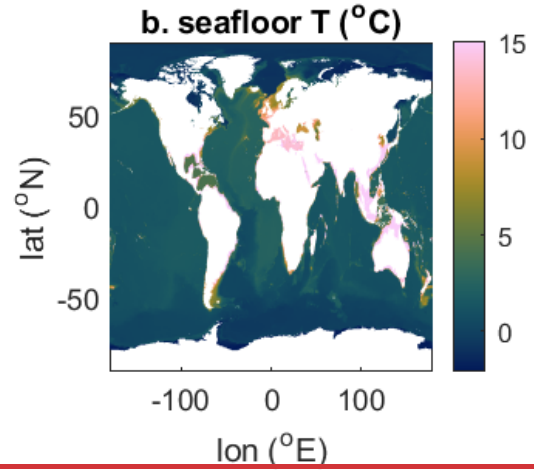
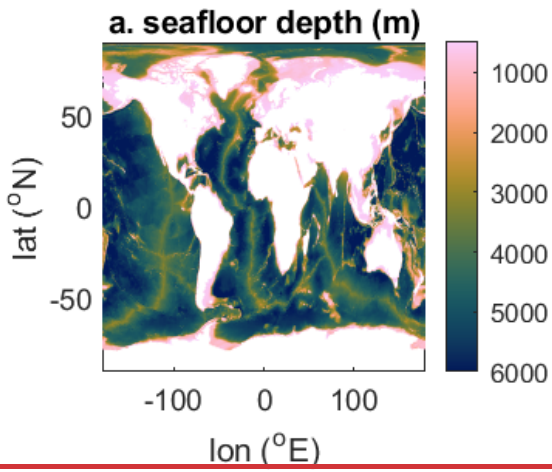
1080
 1081 **Figure 43: Model diagnostics and observational constraints: (a) modelled biomass (gwwt/m²) size distributions for the five sites**
 1082 **using; (b) POC flux estimates from using the Lutz et al. (2007) algorithm (Lutz), from SCOC data (SCOC), from sediment trap**
 1083 **observations (SedTr) and from the model constrained by biomass data from each site (model). Note that sediment trap data are only**
 1084 **available for PAP; (c) model specific rates for maximum net growth (green), respiration (red) and mortality (black) for each of the**
 1085 **5 sites. Note that they differ between sites because of the temperature effect. The two dotted black lines correspond to the constraints**
 1086 **of a maximum growth rate of 0.1 d⁻¹ for the smallest organisms and a lifetime of 50 yr for the largest organisms.; (d) turnover time**
 1087 **(R/POC flux) for each of the 5 sites, estimated using model estimates of R and all observation and model estimates for the POC flux**
 1088 **from (b); (e) a summary table of diagnostic parameters including total biomass (model), R (model), TOC (model and observations)**
 1089 **and biggest organisms' lifetime (model)**
 1090



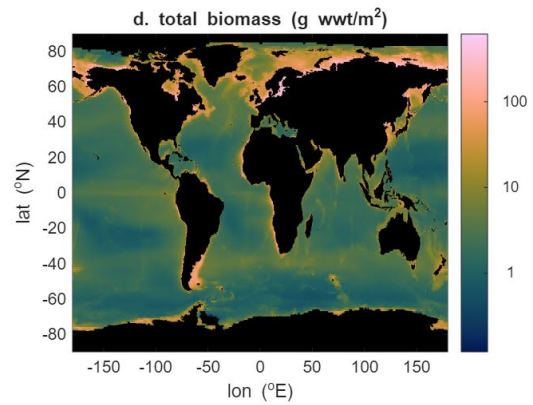
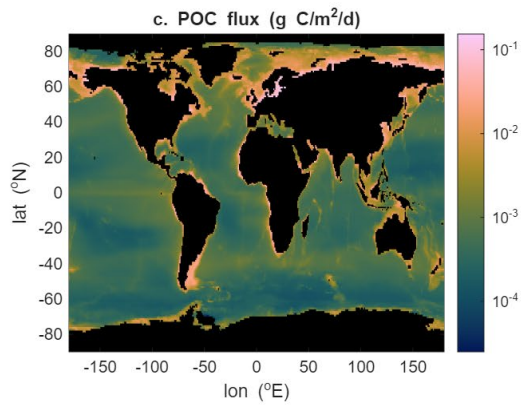
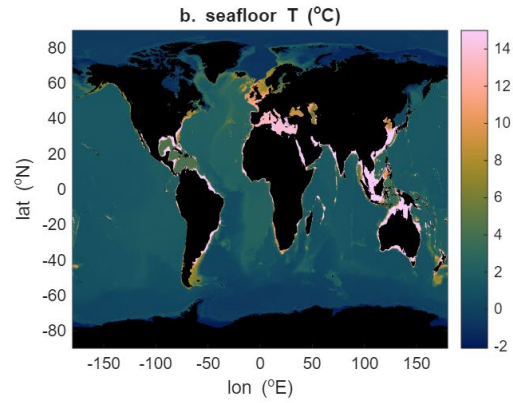
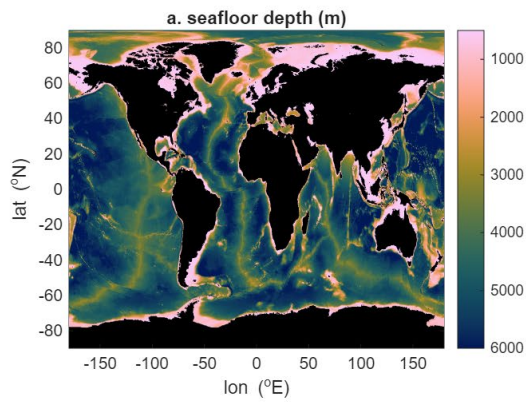
1091 **Figure 5 Sensitivity of the metrics detritus (R), total biomass (ΣB), TOC, turnover time of detritus (T) and lifetime of largest organism**
 1092 **(λ) to each of the model parameters across the five sites. In each case the sensitivity shows the fractional change resulting from a +/-**
 1093 **10% change in the parameter from the standard value. Symbols point in the direction in which the parameter was changed i.e.**
 1094 **upward-pointing pyramids indicate an increase in parameter value and inverted pyramids indicate a decrease.**
 1095

1096

1097
1098
1099



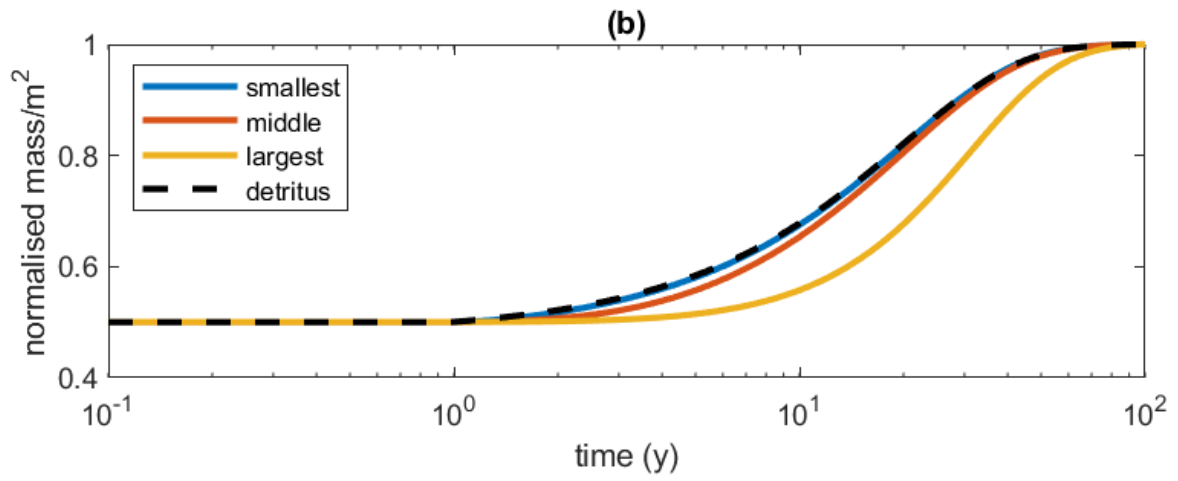
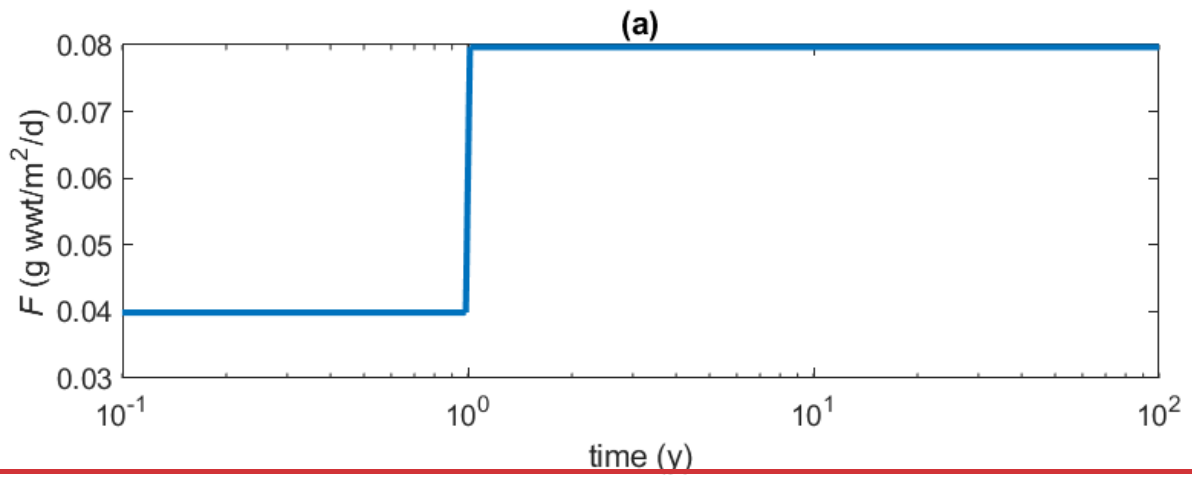
1100



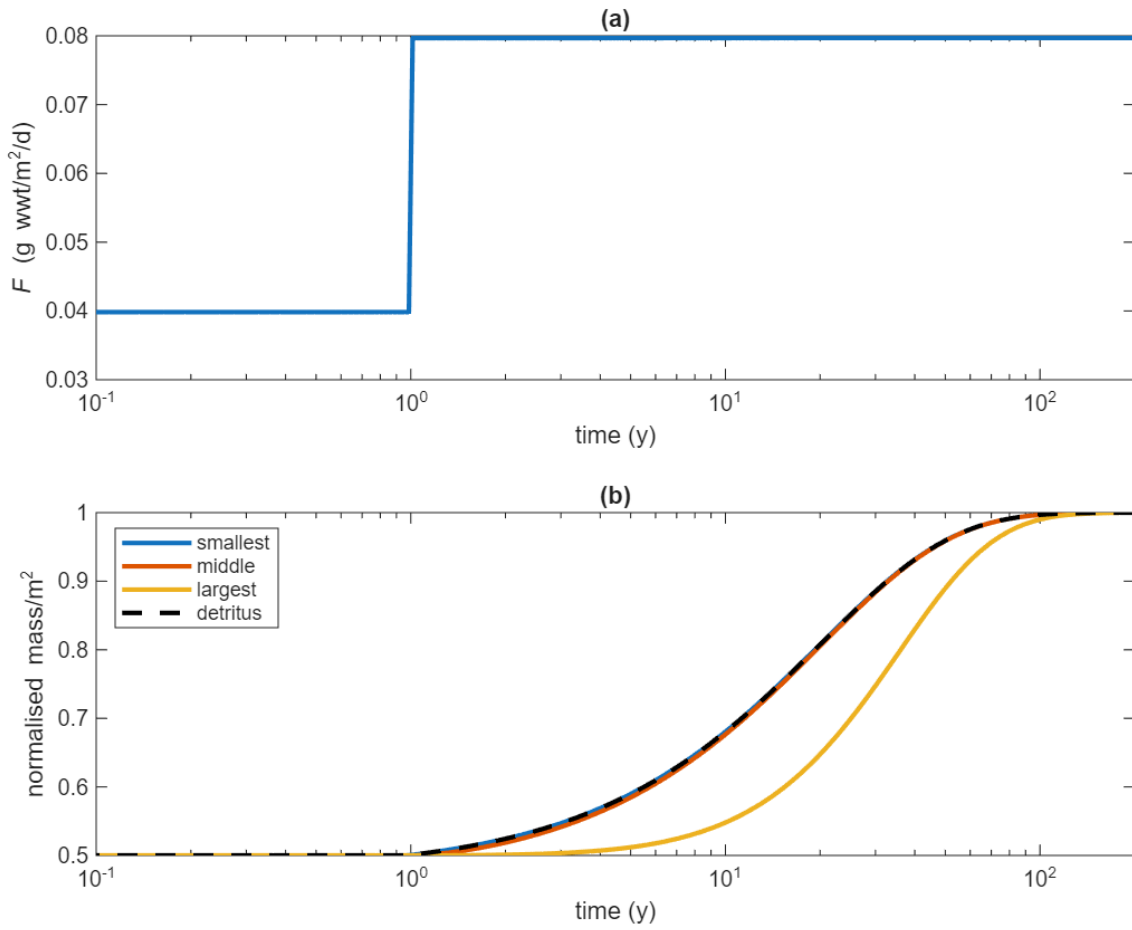
1101

1102 **Figure 64** Example of using the steady state solution (Equations 10 and 11) to explore spatial variability in total benthic biomass:
1103 seafloor depth (a) and temperature (b) from the World Ocean Atlas, particulate organic carbon (POC) flux (estimated using Lutz
1104 et al., 2007) (c), and total biomass (d).

1105



1106



1107

1108 **Figure 75:** Modelled response to a perturbation in which the ecosystem is initially in steady state and then a doubling of the POC
 1109 flux takes place. (a) shows the POC flux, with doubling occurring after 1 year. (b) shows the response of organisms and detritus.
 1110 For clarity only 3 size classes are shown, the smallest, middle and largest ($i=1, 30$ and 59). For the same reason, the biomasses and
 1111 detritus are normalised by dividing by their final value. A log time scale is also used to highlight the different response timescales.

1112

Parameter	Description	Value	Units
g_0	Max. gross-net growth rate at 20°C for organism of size 1 gwwt	0.017	d ⁻¹
r_0	Respiration rate at 20°C for organism of size 1 gwwt	0.0045	d ⁻¹
m_0	Mortality rate at 20°C for organism of size 1 gwwt	0.00053	d ⁻¹
a_0	Interference pre-factor	20500	-
β	Scaling exponent for growth, respiration and mortality	-0.21	-
α	Scaling exponent for interference	-0.26	-
E	Activation energy	0.35	eV

1113

1114

1115 **Table 1: parameter set for BORIS-2**

1116

1117

1118

Site	Lat °N	Lon °E	Depth m	Temp °C	POC flux g C m ⁻² y ⁻¹				TOC g C m ⁻²		R g C m ⁻²
					Lutz	SCOC	Trap	Model	Obs	Model	Model
					CCZ	17.2	-122.6	4150	1.5	0.25	2.9
FG	58.3	0.9	153	8	43	32	-	1654	800	940065	2.6320
FSC	61.9	-2.8	1623	-1	15	5.7	-	3.613	550	550150	0.5275
OM	23.4	59	507	13	8.8	13	-	6.222	2000	200026	1.2130
PAP	48.8	-16.5	4850	2.6	2.5	2.6	1.3	0.4899	320	320200	0.049.9

1119

1120

1121

1122

1123

1124

1125

1126

1127

Table 2: Information on sites from which data were used to constrain parameter values for the general purpose parameter set given in Table 1, together with model diagnostics. POC flux is at the seafloor, estimated using the algorithm in Lutz et al. (2007), SCOC or sediment trap. TOC estimates come from Parameswaran (2024). The “Model” columns indicate model diagnostic values. Model TOC is calculated by assuming that *R* is 5% of TOC. Sources for data are given in Section 2.5